

18th INTERNATIONAL SHIP AND
OFFSHORE STRUCTURES CONGRESS
09-13 SEPTEMBER 2012
ROSTOCK, GERMANY
VOLUME 2



COMMITTEE V.1
**DAMAGE ASSESSMENT FOLLOWING
ACCIDENTS**

COMMITTEE MANDATE

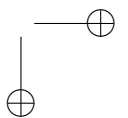
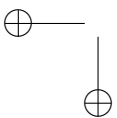
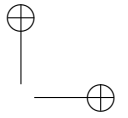
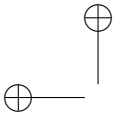
Concern for the structural integrity of offshore structures exposed to hazards. Assessment of risk associated with damage, range of repair required and the effects of temporary repairs and mitigating actions following the damage. The hazards to be considered include hydrocarbon explosions and fires, wave impact, water-in-deck, dropped objects, ship impacts, earthquakes, abnormal environmental actions and possible illegal activities like the use of explosives and projectiles.

COMMITTEE MEMBERS

Chairman: Jerzy Czujko
Natacha Buannic
Sören Ehlers
Chen-Far Hung
Frank Klæbo
Spiro J. Pahos
Mark Riley
Wenyong Tang
Alex Vredeveltd
John Wægter

KEYWORDS

HC Explosions, HC Fires, underwater explosions, wave impact, wave-in-deck, dropped objects, ship impact on offshore structures, earthquakes, abnormal environmental actions, ice and icebergs, flooding, explosives and projectiles



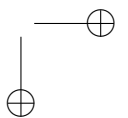
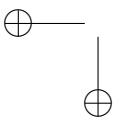
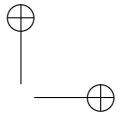
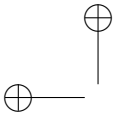
ISSC Committee V.1: Damage Assessment Following Accidents	3
---	---

CONTENTS

1	Introduction	7
2	Hazards on Offshore Facilities	7
3	Hydrocarbon Explosions	8
3.1	Explosion Load Assessment	9
3.2	Load Definition for Design	9
3.2.1	General	9
3.2.2	Overpressure	9
3.2.3	Drag Loads	10
3.2.4	Scenario Definition	11
3.2.5	Probabilistic Explosion Risk Model	11
3.2.6	Generation of Exceedance Curves	12
3.2.7	Design Explosion Loads	13
4	Hydrocarbon Fires	14
4.1	Fire Types. Assessment of Fire Action	14
4.1.1	Gas Jet Fire	15
4.1.2	Pool Fires on an Installation	16
4.1.3	BLEVE	17
4.1.4	Simplified and Early Phase Design	17
4.1.5	Fire Scenarios in Design	17
4.2	Structural Response to Fire Load	18
4.3	Application of Deluge	18
5	Underwater Explosions	18
5.1	UNDEX Load Assessment	18
5.1.1	Experimental Methods for Determining Loading	19
5.1.2	Numerical Methods for Determining Loading	19
5.2	Response Assessment	20
5.2.1	Experimental Response Assessment of Structural Components	20
5.2.2	Numerical Methods – Structural Response	20
6	Wave Impact	21
7	Wave-In-Deck	22
8	Dropped Objects	23
8.1	Loads Assessment	23
8.2	Consequences Assessment	24
8.3	Theoretical Approaches for Pipeline Impact	24
8.4	Numerical FE Approaches	24
9	Ship Impact on Offshore Structures	25
9.1	Loads	25
9.2	Consequences	26
9.3	Literature Study	27
10	Earthquake	28
11	Abnormal Environmental Actions	29
11.1	Freak Waves	29
11.2	Tsunami Waves	29
12	Ice and Icebergs	31
13	Flooding	31
13.1	State-of-the-art	32
13.2	Suggestions for further Research	33

14	Illegal Activities Like Use of Explosives and Projectiles	33
14.1	Terrorist Attack Assessment and Consequences	33
14.2	Definition of Loads	34
15	Design and Assessment Process	35
15.1	Codes and Standards	36
15.1.1	General	36
15.1.2	Robustness	36
15.1.3	Accidental Limit States	36
15.1.4	Designing for Hazards	36
15.2	Risk Assessment Issues	37
15.2.1	General	37
15.2.2	Accidental and Abnormal Actions	37
15.2.3	Framework for the Design Against Accidental Actions	38
15.3	Assessment of Structural Consequences of Accidents	38
15.3.1	Numerical and Simulation Tools	38
15.3.2	Experimental Methods	39
16	Residual Strength/Structural Integrity	39
16.1	Damage Tolerance	39
16.2	Damaged Structures	40
16.3	Mitigation and Repairs	40
17	Material Models for Structural Analysis	40
17.1	Guidelines and Standards	41
17.2	Material Model Database	42
17.2.1	Steel	42
17.2.2	Aluminium	44
17.2.3	Foam, Isolator, Rubber	45
17.2.4	Ice	46
17.2.5	Air	46
17.2.6	Water	47
17.2.7	Explosives	48
17.2.8	Risers, Umbilical or Power Cable	49
17.2.9	Composites	49
17.2.10	Concrete	50
17.2.11	Soil	51
18	Benchmark Study	51
18.1	Scope of Work	51
18.2	Benchmark Model, Geometry	52
18.3	Material data	52
18.4	Loads	52
18.5	Monitoring of Results	53
18.6	Benchmark Procedure	53
18.7	Phase 1 – Modelling Assumptions and Results	54
18.7.1	Modelling Assumptions	54
18.7.2	Summary of Results	54
18.8	Phase 2 – Modelling assumptions and results	55
18.8.1	Unified explosion overpressure	55
18.8.2	Summary of results	55
18.9	Parameter Study	57
18.9.1	Effects of Strain Rate and Material Models Applied	57

ISSC Committee V.1: Damage Assessment Following Accidents	5
18.10 Conclusion from the Benchmark study	57
19 References	58



1 INTRODUCTION

Structural integrity of offshore installations exposed to hazards is one of the challenges offshore industry has faced. Like all kinds of installations, offshore structures can be damaged or collapse as a consequence of a number of possible incidents. For the first time in the history of ISSC activity, a committee has been established to perform a systematic review of offshore installations with respect to their exposure to accidents. The following will be considered:

- The assessment of risk associated with damage,
- The range of repair required,
- The effects of temporary repairs and mitigating actions following the damage.

Therefore, the aims of the committee are to:

- Assess the loads acting on structures during various types of accidents,
- Investigate the consequences of those loads,
- Suggest practical implementation of these findings by establishing balance between structural design and structural safety.

The first step in the project is to identify types of accidents which might occur. Although when it comes to accidents not everything can be predicted, based on statistics and experience, the work is focused on a number of the most probable situations. As expected in the environment where oil and gas are processed, hydrocarbon explosions and fires constitute the most severe hazard for offshore installations. Other extreme conditions this report investigates are: underwater explosions, wave impact, water-in-deck, dropped objects, ship impacts, earthquakes, abnormal environmental actions, ice and icebergs, flooding, as well as illegal activities like the use of explosives and projectiles.

Having established possible threats, the committee's work is to review and recommend best practice in the offshore industry. Ensuring structural safety in the design process of offshore installations requires established procedures for the assessment of loads acting on these structures, as well as procedures for the assessment of the consequences of these loads. Therefore on this level of the project, the focus of the committee is on the following issues:

1. First, the safety measures to be taken during the design phase,
2. Secondly, in case of accidents, the assessment of the level of damage and of the structure's residual strength.

In order to fully investigate the issue of damage assessment following accidents on offshore installations, the committee review selected technical reports and papers worldwide, presenting state-of-the-art research and development achievements in the field.

As part of this Committee's work, a benchmark study has been carried out, aiming at the prediction of structural response of typical offshore installation components subjected to hydrocarbon explosions. The study is based on full scale experiments with hydrocarbon explosions. Its objective is to document how accurately the use of existing software and advanced structural modelling can predict behaviour of structures when subjected to this type of loads.

2 HAZARDS ON OFFSHORE FACILITIES

Quantifying risk in offshore facilities is a multifaceted task as different dynamic effects can arise from various hazards. As deeper oil fields are being discovered, complex

Table 1: Pertinent types of hazards for various offshore facilities

Type of structures	Types of Hazards											
	Explosions	Fires	Underwater Explosions	Wave Impact	Water in Deck	Dropped Objects	Ship Impact	Earthquake	Ice Iceberg	Flooding	Abnormal Environmental Loads	Illegal Activities
Fixed platform	x	x	x	x	x	x	x	x	x		x	x
Semi-Submersible	x	x	x	x		x	x		x	x	x	x
FPSO	x	x	x	x		x	x			x	x	x
TLP	x	x	x	x		x	x				x	x
Spar	x	x	x	x		x	x			x	x	x
Wind turbine, foundation			x			x	x	x	x		x	x

methods of analyses are required. Table 1 is a brief description of a broad range of hazards in offshore facilities and it is by all means not exhaustive. Therefore, engineering judgement must be applied in the design process to select credible hazards.

Identifying the hazards in a tabular format as shown in Table 1 is barely the first step. Predicting the failure modes and any coupled effects likely to arise from secondary or tertiary effects is a challenging task (dropped object > explosion > fire > loss of structural integrity > flooding). Ultimately, any identification will help in preventing and/or mitigating each hazard separately. Feedback from historical data can be of tremendous value during a Hazard Identification brainstorming session (HAZID) when analysing event frequencies and consequences. It is during such sessions that deviations from normal operations, unlikely events, and human factors come into play. Hazards related to offshore facilities are identified by a team of experts and users, who also work jointly on risk assessment, risk reduction and emergency preparedness. These three tasks are separate entities where in most cases the implementation of a risk control option is to be decreed by regulations.

Existing technology can couple numerous scenarios together in a multi-physics analysis where thermal, impulsive, ultimate limit state and hydrodynamic analyses are linked in one common system with the capability of parametric design. Studying various scenarios with advanced techniques can help someone to understand the consequences after the initiating event, and engineer a system against target safety levels.

3 HYDROCARBON EXPLOSIONS

Hydrocarbon explosions and fires are extremely hazardous in offshore installations, Czujko (2010). They involve extreme explosion actions and heat, which have serious consequences for health, safety and the surrounding environment. Since the Piper Alpha accident, a substantial amount of effort has been directed towards the management of explosions and fires in offshore installations. The event scenarios leading to major accidents are generally unpredictable as the calculated frequencies of such accidents are often very low. The consequences of such accidents are however directly related to the inventories of flammable or toxic substances present. To prevent escalation, effective barriers should be in place for the most likely events and a good technical

standard is required for safe operation. Risk-based approaches, rather than traditional prescriptive approaches, have begun to be more extensively applied in offshore designs.

3.1 Explosion Load Assessment

There are no simple calculation methods for determining blast loads for offshore structures. A number of predictive approaches are currently being applied to generate blast overpressure from explosions in congested volumes. However, it is the Computer Fluid Dynamics (CFD) models that are most frequently used for practical offshore development projects. These models solve the underlying equations describing gas flow, turbulence and combustion process topological in precise representation of offshore topsides. Explosion simulations using CFD models have the potential for providing high predictive accuracy and a greater potential of addressing any complex blast scenario.

Other models, such as empirical and phenomenological models, are reviewed and compared in Czujko (2001) and Czujko (2010).

Paik and Czujko (2011b) give state-of-the-art review of technologies used in assessing the risk of hydrocarbon explosions and fires in offshore installations. Both qualitative and quantitative risk assessment approaches are described, and the modelling techniques employed in the quantitative assessment of explosions and fires are presented.

Application of CFD models for calculation of explosion and fire action for FPSO topsides is presented by Paik *et al.* (2011). The existing test data on a methane gas explosion and propane gas jet fire was reanalysed using the ANSYS CFX code. It was concluded that the CFD simulations proposed in this study were in good agreement with the experimental results.

3.2 Load Definition for Design

3.2.1 General

Explosion generates different type of loads depending on the size and shape of structures and equipment. The following types of explosion loads have to be considered in design:

1. Explosion overpressure, p_o , dynamic load generated on large surfaces.
2. Drag force, p_d , dynamic load generated on small equipment items and piping.
3. Differential pressure, p_{diff} , global dynamic load generated on large equipment items or enclosures located within the explosion area by explosion wave passing the object.

Overpressure loads result from increases in pressure due to expanding combustion process. Description of time dependent overpressure and drag pressure is given in Figure 1 and Figure 2.

Drag is a vector quantity in contrast to the overpressure which is scalar, i.e. drag has three independent components. Drag, which is proportional to square of flow velocity, is a significant load for long and slender objects if flow speed in the plane normal to object's length is high. For this reason drag is always measured in a plane, not in a direction, which will be referred to as plane drag. For example drag load in plane XY is significant for objects (pipes) spanning in Z direction etc. (Figure 2).

3.2.2 Overpressure

Module walls, blast and fire walls and decks should be designed to resist explosion overpressures.

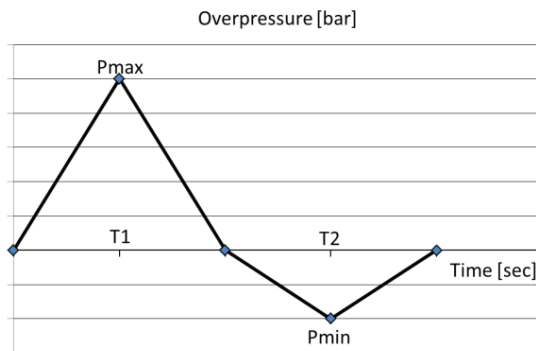


Figure 1: Parameters defining design overpressure and drag pressure

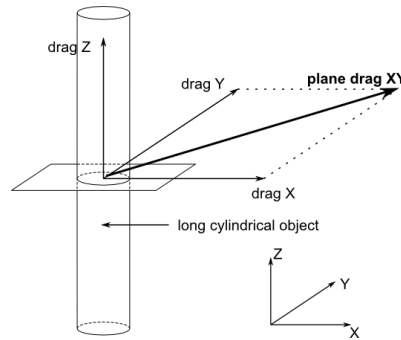


Figure 2: Directions of design drag pressure

For static analysis of walls and decks structure proper Dynamic Amplification Factors (DAF) should be accounted for and applied to increase values of overpressures. When using non-linear dynamic FE method, overpressures can directly be used in the analysis process.

3.2.3 Drag Loads

Drag load is a directional loading due to the passing air/gas flow. Gas explosions can generate both high overpressure and high-speed gas flows as a result of gas combustion process.

According to UKOOA (2003) drag loads dominate for obstacles with dimensions smaller than 0.3 m or on cylindrical obstacles smaller than 0.3 m in diameter, in particular in regions of high gas velocity near vents. Both drag and pressure difference loads are significant on objects between 0.3 m and 2 m in the flow direction. Drag loads are particularly important in open areas such as on the deck structures of an FPSO. The gas clouds associated with explosions on FPSOs may be very large and gas velocities up to 500 m/s could be experienced. The direction of gas flow may also be very variable, for example in the case of the pipe rack of an FPSO acted on by an explosion ignited at low level. Secondary projectiles may be a problem for FPSOs in view of the higher gas velocities.

Drag forces can be represented as, Czujko (2001):

$$F = F_d + F_p$$

Where:

- F_d = Form drag contribution proportional to the area, density and velocity square, and depending on Reynolds number and function of Mach number (U/c), where U is velocity of expanding gas and c is speed of sound.
- F_p = Contribution from the differential pressure.

For small piping and equipment form drag is a dominant contribution in drag forces. Large equipment, as for example compressors, is mainly subjected to effects of differential pressure. Large items like scrubbers are subjected to both drag components. The principles in Table 2 should be used for the calculation of drag force.

Table 2: Limit for equipment size to calculate drag force contributions.

D [m]	F		
	F_d	$F_d + F_p$	F_p
$< 0,6$	×		
$0,6 < D < 2,0$		×	
$> 2,0$			×

3.2.4 Scenario Definition

For an explosion to occur a gas cloud with a concentration between the upper flammability limit (UFL) and lower flammability limit (LFL) must be ignited. The overpressure caused by the explosion will depend, amongst other things, on, API (2006):

1. The gas or gas mixture present
2. The cloud volume and concentration
3. Ignition source type and location
4. The confinement or venting surrounding the gas cloud
5. The congestion or obstacles within the cloud (size, shape, number, location)

Factors affecting the origin of accident events according to Norsok (2010):

- Storage (number and size of inventories)
- Equipment type
- Risers and wells
- Product type
- Ignition sources
- Type of operations
- Production operations
- Deck type
- Structure location

The problems of creating inhomogeneous clouds by dispersion simulations are commonly solved through establishment of equivalent stoichiometric clouds at time of ignition. This may, however, result in a too short duration of the load.

3.2.5 Probabilistic Explosion Risk Model

The explosion risk model considers each leak scenario individually. A leak scenario is described by a transient gas leak rate, gas properties, leak location and direction, and ventilation conditions (wind speed and direction for naturally ventilated areas). For a Total Risk Analysis (TRA) in compliance with NORSOK Z-013 (2010) it is common to apply 9 initial leak rates and 6 leak directions. In addition, 12 wind directions and a range of wind speeds shall be reflected. Normally, the leaks from each process unit are considered individually. This results in a tremendous number of leak scenarios, even if an analysis normally applies a reduced number of wind directions (for which dispersion conditions are similar). The frequencies for the specific leak scenarios are quantified as follows for each process unit:

$$f_{leak\ scenario} = f_{leak} \cdot P_{rate\ and\ fluid\ in\ category} \cdot P_{wind\ direction} \cdot P_{wind\ speed} \cdot P_{jet\ direction}$$

The time dependent leak rate depends primarily on the segment inventory and the blow down system capacity, but also time until the segment is isolated and blow down initiated. A frequency of occurrence is quantified for each leak scenario. The explosion risk is the sum of the explosion risks for each individual scenario.

The HSE Hydrocarbon Release Database (HCRD) is the best quality dataset that exists on offshore releases and has thus become the standard source of leak frequencies for offshore quantitative risk assessment (QRA). Statoil have observed that different solutions by different analysts lead to QRAs having significant inconsistency in leak frequencies despite being based on the same dataset. Statoil therefore initiated a study in 2008 to standardise the leak frequency model to be used for their offshore facilities in the North Sea. Falck (2011) provides a thorough review and presentation of the leak frequency modelling principles established during the study.

3.2.6 Generation of Exceedance Curves

There is currently a lot of industry interest in the generation of curves of the probability of exceeding a specified explosion load at a given location. These curves can relate to overpressure at a point, or averaged over a wall, or other explosion properties such as dynamic pressure or impulse. Exceedance curves are typically plotted on a graph with overpressure plotted on a linear scale on the horizontal axis and annual exceedance frequency plotted on a log scale on the vertical axis. An exceedance curve will always be a monotonically decreasing (discrete) function.

UKOOA Approach

The process provided by United Kingdom Offshore Operators Association (UKOOA) (UKOOA, 2003) is a method of medium complexity for the generation of exceedance curves for the purpose of identification of the design explosion events corresponding to the SLB and DLB. It is advisable to consider space averaged peak overpressures for this purpose as they are more representative of the general severity of the load case. The chosen scenarios will themselves give rise to simulations which have large local variations of peak overpressure.

NORSOK Z-013 Approach

Detailed procedure for generation of exceedance curves is presented in NORSOK (2010).

The procedure described in this document is meant to be used for detailed analyses of platforms in operation or in the project phases where the necessary information on all design elements influencing the risk picture is available. The purpose of the procedure is to standardise the analyses so that the risk of explosions can be compared between different areas, installations and concepts, even if the analyses are performed in different circumstances and by different personnel. Although this procedure is prepared for platforms, many of its guidelines might be useful for generation of exceedance curves for FPSO structures.

Pressure-Impulse Exceedance Surface

Czujko (2001) and NORSOK (2010) recommend generation of Pressure-Impulse exceedance surface instead of pressure exceedance curve, to obtain an improved characteristic of explosion pressure load.

Exceedance Curves for FPSO

A quantitative method for the calculation of explosion risk on FPSO is given in Paik and Czujko (2011c) and Paik *et al.* (2011). The method is a result of a Joint Industry Project on Explosion and Fire Design of FPSO. These procedures can be efficiently applied in offshore development projects, and the application includes the assessment of design explosion and fire loads as well as the quantification of effects of risk control options such as platform layout, location and number of gas detectors, isolation of ignition sources etc.

3.2.7 Design Explosion Loads

Design explosion loads were in the past derived from the worst credible event assuming a gas cloud of maximal extent with stoichiometric composition ignited at the worst time in the worst position. Usually the ultimate peak overpressure derived in this way is far too large to be accommodated by the structure.

NORSOK (2010) defines dimensioning accidental load as the most severe accidental load that the function or system shall be able to withstand during a required period of time, in order to meet the defined risk acceptance criteria. The dimensioning accidental load (DAL) is typically established as the load that occurs with an annual probability of 10^{-4} .

Design accidental load is a chosen load that is to be used as the basis for design. The applied/chosen design accidental load may sometimes be the same as the DAL, but it may also be more conservative based on other input and considerations such as ALARP. Hence, the design accidental load may be more severe than the DAL. The design accidental load should as a minimum be capable of resisting the DAL.

API (2006) and UKOOA (2003) recommend two levels of explosion loading by analogy with earthquake assessment. These are:

- Ductility level blast (DLB) / Design level blast
- Strength level blast (SLB) / Reduced blast load

Low risk installations may be assessed using only the DLB.

The ductility level blast is the design level overpressure used to represent the extreme design event. It is also defined as a low-probability high-consequence event, which must be investigated for at least retaining the integrity of the temporary refuge, safe muster areas and escape routes.

The strength level blast represents a more frequent design event where it is required that the structure does not deform plastically and that the SCEs (safety critical elements) remain operational. It is defined as a higher-probability, lower-consequence event. Performance criteria associated with the SLB may include elastic response of the primary structure, with the safety critical elements remaining functional, and with an expected platform restart within a reasonable period. This load case is recommended for the following reasons:

- The SLB may detect additional weaknesses in the design not identified by the DLB (robustness check).
- An SLB event could give rise to a DLB by escalation – this should ideally not occur as elastic response of SLB and supports should be maintained.
- The prediction of equipment and piping response in the elastic regime is much better understood than the conditions which give rise to rupture. The SLB enables these checks to be made at a lower load level often resulting in good performance at the higher level (strength in depth).
- The SLB is a low consequence event important for the establishment of operability.
- This load case offers a degree of asset protection.

Figure 3 represents an example (simplified) overpressure exceedance diagram. This curve is conventionally plotted with a logarithmic scale for the vertical frequency axis which gives the frequency per year for which the given overpressure will be exceeded. The horizontal axis is a linear scale usually with the peak space averaged overpressure

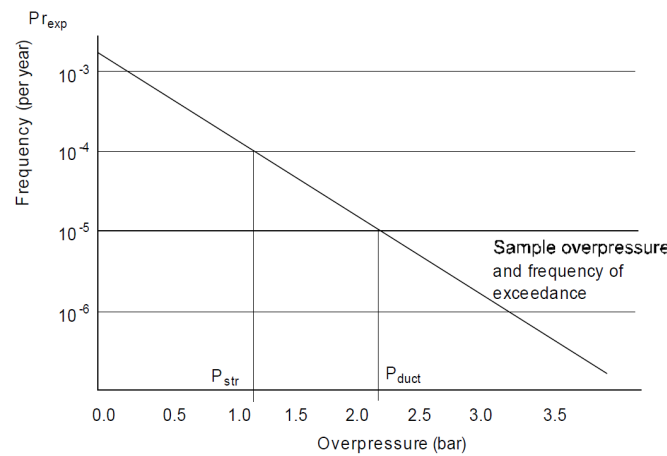


Figure 3: Example overpressure exceedance curve - location of SLB and DLB design load cases (P_{str} and P_{duct})

for the combustion region plotted in bar. This parameter gives a good general measure for the choice of design scenarios. Each of these scenarios may have a large range of local peak overpressures and associated durations within it.

The SLB overpressure, ' P_{str} ' may then be identified as that overpressure corresponding to a frequency one order of magnitude more frequent or with a magnitude of one third of the DLB overpressure, ' P_{duct} ', whichever is greater. The reason for the reduction factor of one third is related to the expected reserves of strength in the structure and the observation that the primary structure will often only experience received loads of this magnitude.

4 HYDROCARBON FIRES

The main purpose of fire analysis of offshore installations is to support risk calculations, particularly verify fire heat to topside structures and smoke exposure to escape and evacuation means.

The fire simulations are typically carried out using the commercial CFD codes as for example Kameleon FireEx, Fluent or Ansys.

The following loads resulting from fire event can be distinguished:

- Radiation from flame to the surroundings
- Convection from the hot combustion products passing over an object surface
- Conduction – not described in this paper, because it is usually small comparing to other methods of heat transfer
- Smoke load (soot and carbon monoxide) formed during an inefficient combustion of hydrocarbons

4.1 Fire Types. Assessment of Fire Action

The most complete classification of fire types, described in UKOOA (2006), comprises:

- gas jet fires
- two-phase jet fire
- pool fires on an installation
- hydrocarbon pool fires on the sea
- gas fires from subsea releases

- BLEVE (boiling liquid expanding vapour cloud explosion)

4.1.1 Gas Jet Fire

An ignited pressurised release of a gaseous material (most typically natural gas) will give rise to a jet fire. A jet fire is a turbulent diffusion flame produced by the combustion of a continuous release of fuel. Except in the case of extreme confinement which might lead to extinguishment, the combustion rate will be directly related to the mass release rate of the fuel. In the absence of impact onto an object, these fires are characteristically long and thin and highly directional. The high velocities within the released gas mean that they are relatively unaffected by the prevailing wind conditions except towards the tail of the fire.

The fire size is predominantly related to the mass release rate which in turn is related to the size of the leak (hole diameter) and the pressure (which may vary with time as a result of blow down). In the case of high pressure releases of natural gas, the mixing and combustion is relatively efficient resulting in little soot (carbon) formation except for extremely large release rates. CO concentrations in the region of 5 to 7% *v/v* have been measured within a jet fire itself but this is expected to drop to less than 0.1% *v/v* by the end of the flame.

Typical characteristics of jet fire are given in Table 3.

Effect of Deluge on Gas Jet Fires

Deluge has little effect on the size, shape and thermal characteristics of a high pressure gas jet fire. Therefore, the heat loading to engulfed obstacles is not diminished. There is some evidence that the deluge increases combustion efficiency resulting in lower CO

Table 3: High pressure gas jet fires, UKOOA (2006).

Characteristic	Unit	Size				Effect of confinement
		Small	Medium	Large	Major	
	kg s ⁻¹	0.1	1	10	>30	
Flame length	m	5	15	40	65	Affected by enclosure shape and openings.
Fraction of heat radiated, <i>F</i>		0.05	0.08	0.13	0.13	
CO level	% <i>v/v</i>	< 0.1	< 0.1	< 0.1	< 0.1	Increased up to 5% at a vent prior to external flaming, but after external flaming < 0.5% at the end of flame.
Soot concentration	gm ⁻³	~0.01	~0.01	~0.01	~0.01	Depends on equivalence ratio from 0.1 gm ⁻³ at $\Phi=1.3$ to 2.5 gm ⁻³ at $\Phi=2.0$.
Total heat flux	kW m ⁻²	180	250	300	350	Increased heat loadings up to 400kW m ⁻² (280kW m ⁻² radiative 120kW m ⁻² convective, $T_f=1600K$, $\epsilon_f=0.75$, $h=0.09$).
Radiative flux	kW m ⁻²	80	130	180	230	
Convective flux	kW m ⁻²	100	120	120	120	
Flame temperature, <i>T_f</i>	K	1560	1560	1560	1560	
Flame emissivity, ϵ_f		0.25	0.4	0.55	0.7	
Convective heat transfer coefficient, <i>h</i>	kW m ⁻² K ⁻¹	0.08	0.095	0.095	0.095	
Effect of deluge		No effect on heat loadings to engulfed objects. In far field, take 1 row water sprays, 2 rows and >2 rows at 12 lm ⁻² . May improve combustion efficiency and reduce CO levels within flame.				Risk of extinguishment and explosion hazard if deluge activated when enclosure is already hot and fire is well established.

and increased CO₂ levels within the flame. The major benefit of area deluge with jet fires arises from the suppression of incident thermal radiation to the surroundings, which protects adjacent plants and, in particular, aids personnel escape. Nozzles producing smaller droplet sizes can have an enhanced mitigation effect, but there is an increased risk that the droplets will be blown away by the wind.

4.1.2 Pool Fires on an Installation

A pressurised release of a hydrocarbon liquid which is not sufficiently atomised or volatile to vaporise and form a jet fire will form a pool. Similarly a spillage from non-pressurised liquid storage will result in a liquid pool being formed. Ignition of the vapours evolving from the liquid can lead to a pool fire which is a turbulent diffusion flame. For hydrocarbons such as condensate the vapours will evolve readily from a spillage and be easily ignited. For heavier hydrocarbons, such as diesel or crude oil, little vapour evolution occurs unless the fuel is heated and hence initial ignition of a spillage may be dependent on the presence of other fires in the vicinity providing sufficient energy to initiate vapour evolution.

Combustion of these hydrocarbons inevitably leads to the production of large quantities of soot, particularly in large pool fires where the size of the pool reduces the ability of air to mix with the fuel evolving in the centre of the pool. The soot emissions result in the characteristic yellow flame and large quantities of smoke can be produced to the

Table 4: Pool fires on the installation.

Characteristic	Unit	Methanol pool	Hydrocarbon pool diameter		Effect of confinement	
			Small	Large		
	m	5	<5	>5		
Flame length	m	equal to pool diameter	twice pool diameter	up to twice pool diameter	Take values as per large hydrocarbon pool fire for worst case. If confinement is severe then mass burning rate will decrease to match available air flow and large external fire at vent is expected.	
Mass burning rate	kgm ⁻² s ⁻¹	0.03	crude 0.045-0.06 diesel 0.055 kerosene 0.06 condensate 0.09 C3/C4s 0.09	crude 0.045-0.06 diesel 0.055 kerosene 0.06 condensate 0.1 C3/C4s 0.12		
Fraction of heat radiated, F		0.15	0.25	0.15		
CO level	% v/v	negligible	< 0.5	< 0.5		Increased CO up to about 5% v/v at a vent prior to external flaming, but after external flaming about 0.5 % v/v at the end of the flame.
Soot concentration	gm ⁻³	negligible	0.5 – 2.5	0.5 – 2.5		Soot levels up to 3 gm ⁻³
Total heat flux	kWm ⁻²	35	125	250	Take values as per large hydrocarbon pool fire.	
Radiative flux	kWm ⁻²	35	125	230		
Convective flux	kWm ⁻²	0	0	20		
Flame temperature, T _f	K	1250	1250	1460		
Flame emissivity, ε _f		0.25	0.9	0.9		
Convective heat transfer coefficient, h	kWm ⁻² K ⁻¹	–	–	0.095		
Effect of deluge		Extinguishable using AFFF. Water soluble but effect of water deluge unknown.	Considerable fire control and potential extinguishment can be achieved. Expect a reduction in flame coverage of up to 90% within 10 minutes. Rapid extinguishment with AFFF. Up to 50% reduction in radiative heat flux to engulfed objects. In far field take F=0.8F for 1 row of water sprays, F'=0.7F for 2 rows and F'=0.4F for >2 rows at 12 l/minm ² .		Expect reduced flame temperatures and reduced or no external flaming. Mass burning rate reduces to match available air flow.	

extent that the smoke can lead to reduced thermal radiation to the surroundings by screening the radiant flame. Hence, the fraction of heat radiated, F , tends to decrease with increasing fire size, although the smoke hazard may increase.

Except in very large fires where buoyancy driven turbulence may become significant, the low velocities within the fire result in the flame being affected by the wind and this factor determines the trajectory of the flame. These low velocities also result in low convective heat fluxes to objects engulfed by the fire; the predominant mode of heat transfer being radiation.

Typical characteristics of pool fires are given in Table 4, UKOOA (2003b).

4.1.3 BLEVE

Fire impingement on a vessel containing a pressure liquefied gas causes the pressure to rise within the vessel and the vessel wall to weaken. Even within a short time, this may lead to catastrophic failure and the total loss of inventory. The liquefied gas which is released flashes producing a vapour cloud which is usually ignited. These events are known as Boiling Liquid Expanding Vapour Cloud Explosions, BLEVEs. This highly transient event generates a pressure wave and fragments of the vessel may produce a missile hazard leading to failure of other items in the vicinity and hence the potential for escalation. In addition, there is a flame engulfment and thermal radiation hazard produced by the fireball.

4.1.4 Simplified and Early Phase Design

In general assessment of fire loads is conducted by analysis of a number of probable fire scenarios. However NORSOK (2008) and DNV (2008) require that the structure is designed for the fire loads shown in Table 5 (unless otherwise documented):

4.1.5 Fire Scenarios in Design

The fire scenario establishes the fire type, location, geometry and intensity. NORSOK (2007) list the following fire scenarios that should be considered:

1. Burning blowouts in wellhead area
2. Fire related to releases from leaks in risers, manifolds, loading/unloading process equipment, storage tanks
3. Burning oil on sea
4. Fire in equipment on electrical installations
5. Fire on helicopter deck
6. Fire in living quarters
7. Pool fires in deck or sea

According to UKOOA (2003), the following specific considerations should be taken into account when defining fire scenario for an FPSO:

Table 5: Heat flux values, NORSOK Z-013.

Storage in an area	Design loads
Both gas containing equipment and oil containing equipment	<ul style="list-style-type: none"> • jet fire 250 kW m^{-2} for 30 minutes • pool fire 150 kW m^{-2} for the following 30 minutes
Only oil or condensate containing equipment	<ul style="list-style-type: none"> • pool fire 150 kW m^{-2} for the following 60 minutes
Only gas containing equipment	<ul style="list-style-type: none"> • jet fire 250 kW m^{-2} for 30 minutes

1. Oil storage tanks – may present hazard in the form of either large scale storage of stabilised crude or with empty storage tanks containing potentially explosive mixtures.
2. Non-process hydrocarbon inventories – The FPSO is a power-hungry installation and requires substantial stores of diesel to maintain station, process utilities power demands plus other life-supporting systems. The vessels are often located in difficult or remote places and will generally be designed to be “self-sufficient” for extended periods in the event that supply vessels cannot reach them.
3. Jet fires on main deck – The process decks on FPSO are often lifted clear of the cargo storage tank, a 5 m gap is not uncommon. The space provided also allows jet fires from the underside of the process to reach other process or utility modules without any impingement to reduce the effect of the flame.
4. Offloading and pool fires on the sea – Offloading to shuttle tankers is a regular event and poses a significant risk both on the FPSO and the shuttle tanker. The risks comprise the breakage or leakage of the transfer hoses and the potentially flammable mixing of hydrocarbon and air in the storage holds of FPSO and shuttle tanker. During the offloading operation, the shuttle tanker and FPSO are in relative proximity and the risks on either vessel are compounded by increased potential for escalation to another vessel.

4.2 Structural Response to Fire Load

Kim *et al.* (2010) have presented a study evaluating the load characteristics of steel and concrete tubular members under jet fire, with the motivation to investigate the jet fire load characteristics in FPSO topsides. ANSYS CFX, and KFX codes were used to obtain similar fire action in the numerical and experimental methods. The results of this study provide a useful database to determine design values related to jet fire.

4.3 Application of Deluge

Many international standards specify firewater deluge rates intended to protect personnel from thermal radiation from the fires during escape, and to cool equipment and structures affected by thermal radiation or direct flame impingement. Application and limitations of existing standards ISO 13702 and NFPA15 are discussed by Madonos and Ramm (2009). The assessment reveals that current standards are generic and in specific cases the application of these standards may lead to an unsafe design of deluge systems.

5 UNDERWATER EXPLOSIONS

After seeing the effects of UNDEX and surface explosions on various ships, such as the USS Cole, Superferry 14 and Limburg it would be very likely to predict similar attacks on offshore structures and platforms such as semi-submersibles, FPSOs, TLP, Spar, or offshore wind turbines. In order to determine the influence of such events this section examines structural response and loading characteristics for underwater explosions.

5.1 UNDEX Load Assessment

Underwater explosions result in loading mechanisms which exhibit significantly different time scales and loading. Initially a high pressure shockwave radiates from the point of detonation after which the explosive products form a superheated, highly compressed gas bubble. The gas bubble expands until the internal pressure becomes smaller than the ambient hydrostatic pressure at the depth of the detonation at which point it will collapse. These events are shown in Figure 4.

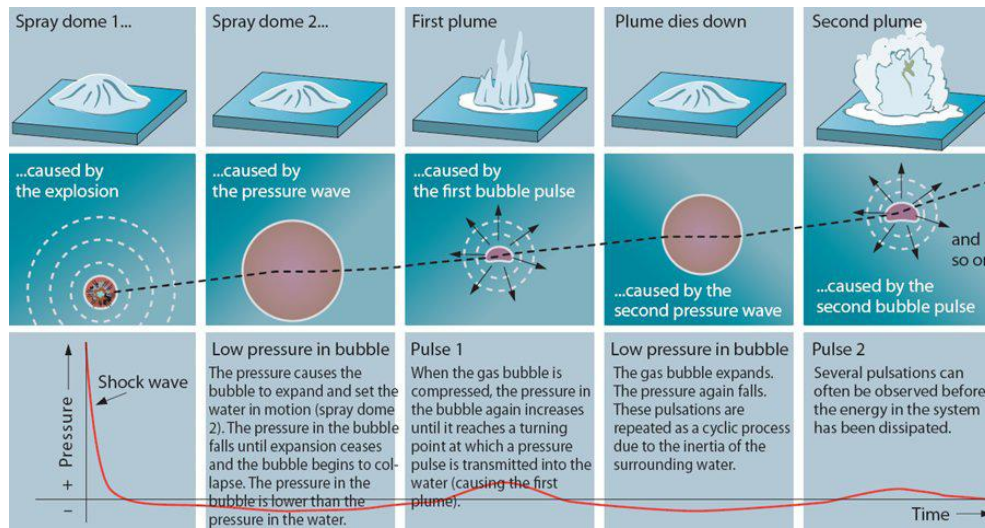


Figure 4: Stages of shock wave and the pressure effect on the sea surface

5.1.1 Experimental Methods for Determining Loading

Lee *et al.* (2010) performed experiments on rigid target plates in order to determine the behaviour in the loading of the bubble collapse at varying standoffs. They found that the bubble collapse loading increased with an increasing standoff up to approximately $0.8R$ at which point the load decreased, as shown in Figure 5. This also shows the bubble collapse impulse loading is significantly larger at close standoffs than the shock impulse loading.

5.1.2 Numerical Methods for Determining Loading

The most likely UNDEX event to occur on offshore structures is a close proximity event. The numerical approach would include a meshed model using a CFD or hydrocode model. Riley *et al.* (2010) performed simulations of the rigid target experiments that were conducted by Lee *et al.* (2010). The numerical simulations were conducted with the CFD code Chinook, which is developed and distributed by Martec Ltd. Simulations were performed for all experimental standoffs, 0.2 times the maximum gas bubble radius, R , up to a standoff of $2R$. The Chinook load predictions

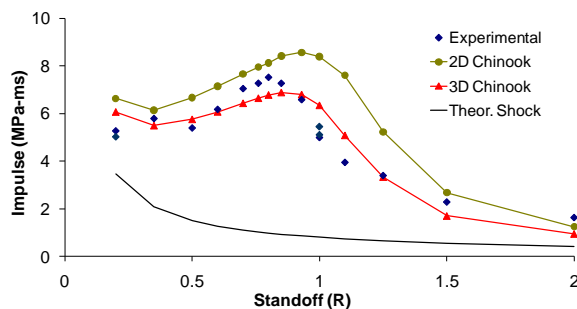


Figure 5: Comparison of experimental and numerical bubble collapse loads along with the theoretical shock loading for rigid plate experiments conducted at DRDC Suffield (Riley *et al.*, 2010)

were found to be qualitatively correct; however quantitative gaps remain, as shown in Figure 5.

5.2 Response Assessment

Determining the structural response for UNDEX can be very time-consuming and costly. Techniques used to determine the structural and operational integrity for offshore structures due to UNDEX events can be performed using numerical and/or experimental methods.

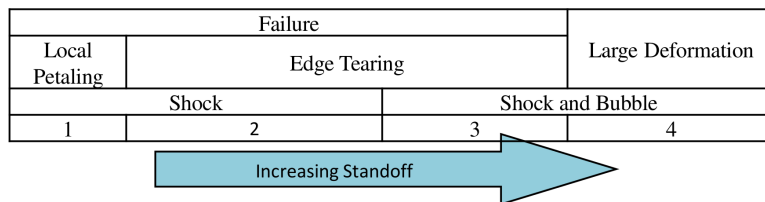
5.2.1 Experimental Response Assessment of Structural Components

Lee *et al.* (2008) showed the result of an extensive experimental close-proximity UNDEX assessment on small scale plate targets. The failure regimes that were determined from the experimental program are outlined in Figure 6.

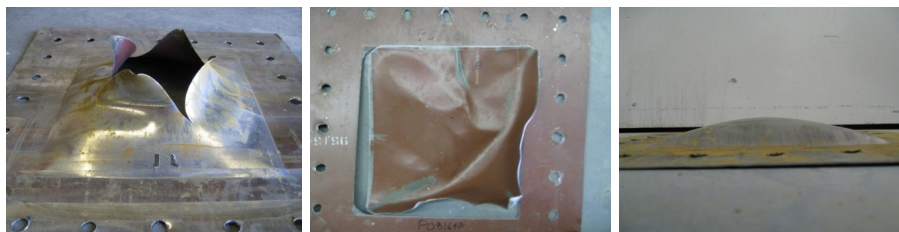
5.2.2 Numerical Methods – Structural Response

Hung *et al.* (2009) studied the nonlinear dynamic response of cylindrical shell structures subjected to underwater explosion loading through experiments and numerical simulations implementing USA/DYNA software. For far-field UNDEX cases the accelerations and strains from the FE analysis showed good agreement with the experiments. For near-field cases the results were qualitatively correct, however quantitatively there were considerable differences.

Zhang and Yao (2008) used a coupled BEM and FEM to calculate the coupling between the gas bubble and a structure. The toroidal bubble method developed by Wang *et al.* (1996a, 1996b) was implemented, which was expanded to three-dimensions by Zhang *et al.* (2001). Zhang and Yao calculated the response of a submerged cylinder to the bubble pulsating pressure, retarded flow, and the jet, and compared to experimental results. The error in numerical approach was found to be approximately 10%. They



(a)



(b)

(c)

(d)

Figure 6: Failure regimes determined from small scale experiments conducted at DRDC Suffield (a) Failure regimes as a function of standoff, (b) local petaling failure (zone 1), (c) edge failure (zones 2 and 3), (d) large deformation (zone 4) (Lee *et al.*, 2008)

Table 6: Critical standoff range where failure occurs in the plate specimens (Lee *et al.*, 2008, Dunbar *et al.*, 2009)

Charge	Plate Thickness	Numerical Range	Experiment Range
20 g C4	1.21 mm	0.69R – 0.75R	0.75R – 0.85R
20 g C4	0.76 mm	1.10R – 1.15R	1.15R – 1.25R
50 g C4	1.21 mm	1.06R – 1.15R	1.06R – 1.50R

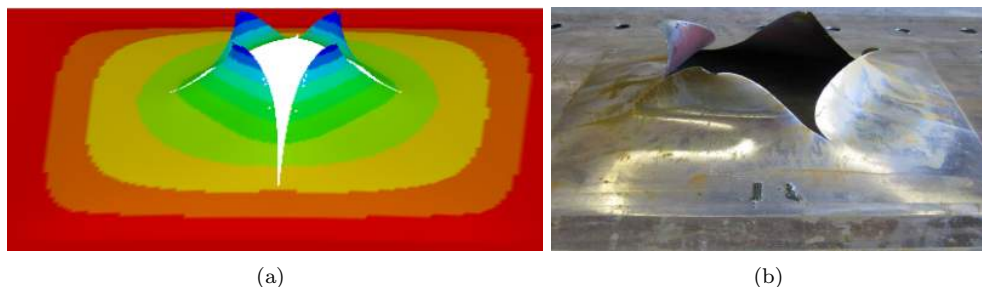


Figure 7: Plate failure from contact charge, (a) numerical prediction (b) experimental results

also showed that ship motion is linked to the phase of the bubble, so that there is a suction force as the bubble starts to collapse, causing ship to sag and putting it in a very vulnerable position for bubble collapse.

Dunbar *et al.* (2009) performed simulations of the small scale target experiments that were conducted at DRDC Suffield by Lee *et al.* (2008). Their results were compared to the ranges observed in the experiments, as shown in Table 6.

Riley (2008) simulated contact/near contact charges to determine the failure limits for centre plate punch-out failure in small scale targets using LS-DYNA and compared them to the experiments conducted at DRDC Suffield. It was found that through thickness shear stress is the dominate failure initiation mechanism for contact/near contact charges. The predicted failure pattern in the targets was found to agree reasonably well with the experiments, as shown in Figure 7.

Recent studies such as that by Yao *et al.* (2009) showed that the conventional shock factors have deficiencies in their ability to reflect the equivalency of structural explosive environments resulting from underwater explosions. Yao *et al.* proposed a new shock factor based on a spherical wave and the area of the structure normal to the wave propagation, S_E , which is a modification of the traditional shock factor C_2 , Eq. (1). Their results showed that their proposed shock factor significantly reduced the variations in the structure kinetic and potential energies for constant shock factors with varying charge weights and standoffs.

$$C_3 = \sqrt{S_E} C_2 \quad (1)$$

6 WAVE IMPACT

For many offshore structures wave impact loads is a design consideration that can influence both the required strength and, especially for ships and floaters, also the in service behaviour.

For ship-shaped structures and other floaters both steep waves impacting the bow and extreme loads due to wave breaking against platform columns may be important

design considerations. In Voogt (2004) it is thus reported that damage from wave impact loading has been experienced by several FPSOs. It also describes some results from the project SAFE-FLOW, where a design evaluation method to investigate bow impact from steep waves was developed. In Helland (2001) the development of a design tool for prediction of loads and responses due to impact from steep waves on ships and platforms is reported. The work is largely based on existing tools validated by model testing and calibration. The practical outcome of the project is a software package for practical engineering use.

A comparison between impact loads due to breaking waves obtained using an available (DNV) recommended practice with results from model tests is presented in Suyuthi (2009). The comparison was not made on an event by event basis, but rather on a q -probability wave impact load level for impact forces against platform columns. The conclusion was that the recommended practice is in reasonable agreement with model test for $q = 10^{-2}/year$, whereas model test results suggest larger impact loads than the recommended approach for $q = 10^{-4}/year$.

7 WAVE-IN-DECK

For fixed offshore structures wave-in-deck loads are becoming of increasing importance, especially for such steel jackets where subsidence has reduced the clearance between the underside of the deck structure and the sea surface to a critical magnitude.

Although the required clearance between the sea surface and the underside of the deck is a design parameter that is always carefully evaluated in any jacket design, more compaction of the reservoir than anticipated sometimes has taken place, and higher wave crests than originally anticipated have been experienced. This leads to a situation where the effective water depth is increased and in some cases to such an extent that the underside of the deck is impinged by large waves. This leads to an additional large wave load from the wave hitting the deck that was not anticipated during the original design, and thus typically is critical to both the deck structure and the support structure.

Current developments are directed towards a better prediction of both the subsidence and a refined prediction of abnormal wave crests that may impinge on the deck structure. In new designs the designer uses an additional safety margin on the calculated required minimum distance between the sea surface and the underside of the deck structure in terms of an air gap requirement. A state-of-the-art procedure to determine the required deck elevation can be found in ISO 19902 (2007).

For those fixed jacket structures that are in danger of experiencing wave-in-deck loads from waves with a return period of the order of 10,000 years or lower, wave-in-deck load becomes a design consideration. Such structures have been investigated in Van Raaij (2005 and 2007). These investigations focus on estimation of wave-in-deck loads on jacket structures in the North Sea for the rare 10,000 year event, especially on horizontal loads. They conclude that there is no general consensus on which method to use to calculate wave-in-deck loads. Further, a distinction is made between two main approaches: 1) the global or the silhouette approach (e.g. API and ISO) which use an effective deck area exposed to the pressure from the water particles, and 2) the component approach (e.g. Kaplan) in which loads on single members are calculated separately and finally added. Such methods typically determine the maximum wave-in-deck load which may be used directly for static analysis. However, it has been found that dynamics sometimes become important and may help the platform to survive,

particularly if the platform is sufficiently ductile. Therefore, a time history of the wave-in-deck load is needed in addition to the maximum value.

Both (Van Raaij, 2005 and 2007) conclude that vertical wave-in-deck loads are of considerable magnitude and therefore should be considered together with coexisting horizontal wave-in-deck loads. However, the actual detailed investigations are restricted to the horizontal wave-in-deck loads.

For the horizontal wave-in-deck load Van Raaij (2007) recommends to use a generic load time history based on a non-dimensional time found as real time divided by a basis load duration and a reference load. This procedure is intended for analyses where detailed information on the deck load is unavailable, and where a simplified 'rough-but-reasonable' estimate can be accepted. However, it should be noted that since this approach does not determine a co-existing vertical wave-in-deck load it does not constitute a complete design tool.

8 DROPPED OBJECTS

Daily lifting operations of any lifted object entails the risk of the object being dropped on the topside or sub-structure. Therefore, the associated risk is assessed based on a daily basis prior to the site-specific lifting operations. A typical risk assessment of dropped objects includes the analysis of the probability, also using statistics, as well as the structural consequences. Therefore, the object to be lifted by cranes and the operational area need to be identified. Furthermore, it is not the damage of a deck itself (e.g. by permanent deflection) that poses a threat during hydrocarbon fire, but the possibility of equipment damage below the deck. Consequently, the aim of a dropped object assessment is the protection of the equipment rather than the structure. Another threat is a dropped object, such as a container, which may bounce off the deck and roll into an unprotected area. Additionally, structural damage may occur when objects like brackets for jackets or pressurised tanks are lifted over the deck. Furthermore, crane booms may collapse to the deck or objects may strike a pipeline or subsea installations.

DNV and Norsok give some recommendations concerning loads and consequences of dropped objects.

Recommended Practice DNV-RP-F107 (DNV, 2001) presents a risk-based approach for assessing pipeline protection against accidental external loads. The DNV document proposes a classification for typical potential dropped objects as well as a classification for damage and assesses the energy absorbed by the impacting pipe with a simple analytical equation.

Norsok N-004 (2004) summarizes formulae for determination of the impact velocity (in air and in water), as well as formula for the strain energy dissipation and the associated damage (indentation or failure).

8.1 Loads Assessment

Typically, the load assessment is a result of a case-by-case risk analysis considering the frequency of occurrence, because there are no rules for the dropped object type. In other words, the risk assessment provides the scantlings of the dropped object and the operational area (target deck and/or plate) as well as the available kinetic energy. Additionally, a selection of possible loads can be found in OTO 2001 013 (HSE, 2001).

8.2 Consequences Assessment

At first, it can be noted that no guidelines for allowable consequences exist, yet NOR-SOK N-004 presents some allowable deformations on structure in terms of energy limits, but no measures for consequence control are provided.

Consequently, the shape, stiffness, orientation, mass and fall height of the dropped object are important parameters and it is necessary to assess them using a case-by-case risk assessment in line with the aforementioned load assessment.

Therefore, a conservative approximation typically utilizes a rigid indented, dropped objects respectively, to impact the operational area. The applicability of this approximation is however questionable and it may not be sufficient. Furthermore, besides the local impact, the global structural deformations may need to be considered, as well as the support effects. The latter may be addressed with analytical formulae; however, a direct simulation approach would be favourable.

8.3 Theoretical Approaches for Pipeline Impact

Besides the simplified indenter geometry, the support boundary conditions of the pipe resting on the soil need to be accounted for, whether it is simply supported, fixed or realistically somewhere in between these theoretical conditions. Therefore, DNV (2001), Wierzbicki and Suh (1988) and Ong and Suh (1996) provide simplified formulae for different boundary conditions.

Furthermore, Poonaya *et al.* (2007), Thinvongpituk *et al.* (2008) and Alashti *et al.* (2008) are concerned with the bending load of the pipe during the impact and propose formulations for ultimate bending moment rather than for dent depth.

Ong and Lu (1996) and Famiyesin *et al.* (2002) utilize the finite element method to obtain a range of results for different boundary conditions, which they utilize to obtain semi-empirical equations through curve fitting.

8.4 Numerical FE Approaches

FE-methods concentrate mostly on the assessment of the multitude of the possible scenarios of dropped objects and structural configurations to be analysed. An FE-analysis is the most flexible method and can account for the possible effects occurring and to assess the following relevant factors:

- Impact energy (constant drop height + variation of dropped object mass)
 - Dropped containers: post dropped object response: bouncing or rolling requires explicit FE-codes (contractual time limits often prohibit this phase, even though it can influence consequences significantly)
- Boundary conditions
 - Support stiffness, Length between supports, Internal pressure in pipes
- Material
- Discrete indenter shape and stiffness
- Indentation location

Although a drop test is typically of a low-speed impact, the short duration of this event and the nonlinear response of the interacting parts, with flexible stiffness behaviour, require the use of an explicit FE solver. It is also important to carry out the drop test at a series of impact angles as highly localised deformation can take place at certain angles. The material properties in the FE model will need to account for work hardening and implement the appropriate failure model, see also Chapter 17 on material modelling.

9 SHIP IMPACT ON OFFSHORE STRUCTURES

Over the past decades, the structural engineering design community has increasingly applied risk assessment methodologies for ship and offshore collision problems. The ISSC 2006 V.1 committee recommended risk assessment methodology to be more widely and frequently applied in analyses, and that structural crashworthiness be explicitly taken into account.

In the design of ships, risks due to collisions and grounding are in general not explicitly considered, except in specific cases. On the other hand, the offshore industry has a risk management concept that is significantly different from that of the marine industry. The offshore industry use systematic assessment procedures for fixed platforms that address the probability of occurrence, risk ranking, structural analyses, and acceptance criteria, see API (2000). Risk assessment methodologies are discussed in detail in Chapter 15: Design and assessment process.

Given that the collision event takes place, the loads and consequences of the collision event must be determined. A number of analysis tools and procedures for collision analyses have been developed and presented during the last decades. The current chapter gives an overview of common deterministic principles and methods applied in analysis of ship and offshore structures collisions.

The main concern in ship impacts on fixed platforms is the reduction of structural strength and possible progressive structural failure. However, the main effect for buoyant structures is damage that can lead to flooding and, hence, loss of buoyancy. The measure of such damages is the maximum indentation implying loss of water tightness. However, in the case of large damage, reduction of structural strength, as expressed by the indentation, is also a concern for floating structures.

9.1 Loads

In ship impacts on offshore structures, the loads are governed by the kinetic energy of the striking ship. The kinetic energy may be estimated from the mass of the ship, including the hydrodynamic added mass, and the speed of the ship at the instant of impact. If the collision is non-central, a part of the kinetic energy may remain as kinetic energy after the impact. The remainder of the kinetic energy has to be dissipated as strain energy in the installation and in the vessel. Generally this involves large plastic strains and significant structural damage to either the installation, the ship or both. The mass of the offshore structure is usually much larger than the striking ship, and most kinetic energy will be dissipated to strain energy.

The collision event is a complex interaction between vessel motion, offshore structure motion, interaction with the fluid, global hull response in the ship and offshore structure, inelastic deformations in both structures, friction etc. A common, simplified approach is to split the problem into two uncoupled analyses; external mechanics and internal mechanics. The external mechanics analysis uses global inertia forces and hydrodynamic effects to estimate the amount of kinetic energy available to be dissipated to strain energy during collision. The internal mechanics analysis calculates the energy dissipation and distribution of damage in the two structures.

The external dynamic analysis is able to predict the motion of the vessel and offshore structure in the surrounding water during the collision event. The goal of the analysis is to estimate the fraction of the initial kinetic energy which will be released for plastic deformation and rupture in the ship and offshore structure. Several methods are available; full time-domain analysis, simplified analytical methods, simplified formulas

from rules, ex. NORSOK (1998). Zhang (1999) showed that external mechanic methods developed for ship-ship collisions may in general apply to ship impacts on offshore structures as well. However, offshore structures are usually moored, which can give different external mechanics characteristics from those of ship-ship collisions.

Several assumptions are required to split the problem into two individual problems; negligible interaction between the global movement and local plastic deformation, dominant inertia forces, no damping, etc. Hence, the uncoupled analysis methods can only predict the penetration for few conditions correctly. Arbitrary collision angles, sliding and different mass ratios are generally difficult to capture and these methods can only predict the response with high accuracy in symmetric collision events.

Efficient coupled dynamic collision simulation methods are available and are able to take the ship motion and structural deformation and their interaction into account simultaneously. Coupled methods will in general provide a better energy correspondence and increased accuracy. Pill and Tabri (2009) present an efficient and robust method for coupled dynamic analysis in LS-DYNA. The method considers the most important force components accurately; the inertia force and contact force. The ship motions are limited to the horizontal plane which enables neglecting the restoring force, buoyancy and gravity, which are not straightforward to include. Similar methods are available, but the advantage of the proposed method is that special user subroutines are not required, and only conventional tools are used.

9.2 Consequences

The consequence of the collision is dependent upon numerous parameters, but the most important factor is the energy released during the collision event. In split methods, the results from the external mechanics analysis may be compared to the absorbed energy vs. penetration curve found from the internal mechanics analysis. Integrated approaches take both into account simultaneously, and at a higher accuracy.

The analysis methods of internal mechanisms can be categorized into four groups; Simple formulae, Simplified analytical approach, Simplified FEM and Non-linear FEM simulation.

The simple formulae are mostly used to estimate the initial energy absorption. Simple formulae have been developed for a wide range of problems, including head-on collision, grounding and ship-bridge collision.

Simplified analytical approach may be used to calculate the initial energy absorption and loads. This group of methods may estimate the basic characteristics of structural crashworthiness with minimized structural modelling efforts. Applications of this methodology to various collision and grounding situations were summarized extensively by the ISSC 2003 Committee V.3.

Non-linear FEM simulation is the preferred choice for advanced and accurate analysis of collision events. Progress in software development and hardware technology has enabled advanced non-linear analyses including large deformations, sophisticated non-linear material models, complex and robust contact algorithms and more accurate modelling of rupture. Several commercial non-linear FE-solvers are available and commonly used for collision analysis. Non-linear FEM simulations have become standard, and numerous examples have been presented in conference proceedings. The selection of elements, meshing, loads and boundary conditions have become more straightforward because of extensive development in commercial software codes. The material definition and selection is still a major challenge, especially with respect to prediction

of ductile crack initiation and propagation. Several models and methods have been proposed and used with success lately, see Chapter 17 for details.

A simpler approach is to utilize force-deformation curves. NORSOK (1998) Appendix A, includes recommended design curves for supply vessels for various scenarios. The code includes characteristic force-deformation curves for tanker (i.e. FPSO) bow impact as well.

Simplified, analytical methods may also be used to estimate the damage. These can be divided into three classes; empirical methods, analytical plastic methods and analytical buckling methods. The empirical methods relate the energy dissipation to the volume of the damaged material in the offshore structure and striking ship. This may be used to establish a relationship between the intrusion depth of a structure and the amount of absorbed energy for ships at collision. The analytical plastic methods calculate the entire crushing process, and will assess the average collision force. The method assumes that the structure is built from a few fundamental components. The energy dissipation for each component is estimated and the total energy dissipation is found by summarizing for all components.

The analytical buckling method assumes that the maximum strength of a component may be calculated from the plate slenderness factor of basic components. The slenderness factor is found by reducing the cross section to flat flange elements.

9.3 Literature Study

Isshiki *et al.* (2010) presents a model where the struck ship is replaced by a system composed of rigid bars and elasto-plastic hinges. This model not only can express the response of the struck ship more reasonably, but also does not require much time for numerical simulation.

Hogstrom *et al.* (2010) presents Finite Element analysis of a ship-to-ship collision scenario, where the damage opening of a struck ship is simulated for a selection of damage degradation models and realistic material properties. Both the model and material properties include uncertainties. A holistic approach is developed, combining structural integrity and damage stability research with the use of a systematic parameter (sensitivity) and collision-scenario-based analysis.

Hu *et al.* (2010) study a collision scenario in which a moored semi-submersible is struck by a containership through the model test, simplified analytical method and numerical simulation. Two special devices, Ship Launching Device and Energy Absorbing Device are used for the model test. It is shown that the prediction by a NTNU in-house program developed by simplified analytical method is consistent with the results by the model test. And then, it is shown that the collision force dominates the accidental moment, and that the tension forces of the mooring lines are much smaller than the collision force, with an obvious lag behind.

Qiu and Grabe (2010) carry out Finite Element analysis using a Coupled Eulerian Lagrangian approach in order to simulate the collision experiment of waterway embankments of inland waterways with an experimental ship. The stopping distance and the reaction force obtained by the numerical simulation shows good agreement with the field test results. The effects of initial velocities and bow types of the ship on the collision process are also investigated.

Lin *et al.* (2010) show how FEM is used to simulate the collision process of two submersibles. Stress and strain distributions, collision forces, and plastic energy absorption are obtained. The motion lag of the struck submersible in the collision process is

discussed and it is found that it is sensitive to impact velocity which increases with the increase of velocity.

10 EARTHQUAKE

The earthquake induced loading of an offshore structure can cause severe structural damage due to the ground accelerations or as a result of subsidence. Hence, according to NORSOK standard N-003 earthquake actions should be determined based on relevant tectonic conditions and seismological time histories describing further earthquake motions including peak ground accelerations at the site in question. In the absence of such information, the peak ground acceleration at annual exceedance probabilities of 10^{-2} and 10^{-4} given in seismic zonation maps in NFR/NORSAR (1998) can be applied.

However, in severe cases like the 3.11 disaster in Japan, those measures would have failed, because the intensity of the earthquake (M 9.0) surpassed previous measurements, and the occurrence of more than 400 aftershocks with $M > 5.0$, wherefrom five aftershocks with $M > 7.0$, contributed to the damage, see Figure 8. Consequently, the soil-structure interaction as a result of the subsidence of up to 5.3 m horizontally and 1.2 m vertically would not have been predicted sufficiently based on history measurements, see Figure 9.

Typically, earthquake design includes an ultimate strength check of relevant components as well as accidental limit state check of the overall structure to prevent collapse during the earthquake; for details see for example NORSOK N-001.

Furthermore, structural action effects may be approximated using simplified response spectra, also considering different soil conditions for specific seismic zones. Additionally, before any detailed analysis is carried out, an estimate of the global force based on a single dynamic mode of the response spectrum may justify its necessity. However, such simplified analysis may be limited to the underlying soil conditions and this has to be judged on a case-by-case basis due to the large regional variations, see Chapter 17.3 for soil materials and the references there in. For details on structure-soil interaction see Clouteau *et al.* 2012 and Menglin *et al.* 2011. Furthermore, the structural

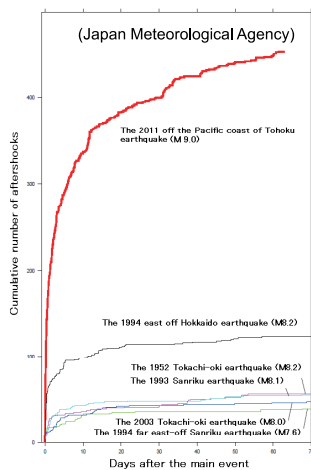


Figure 8: Cumulative number of aftershocks (Fujita, 2011)

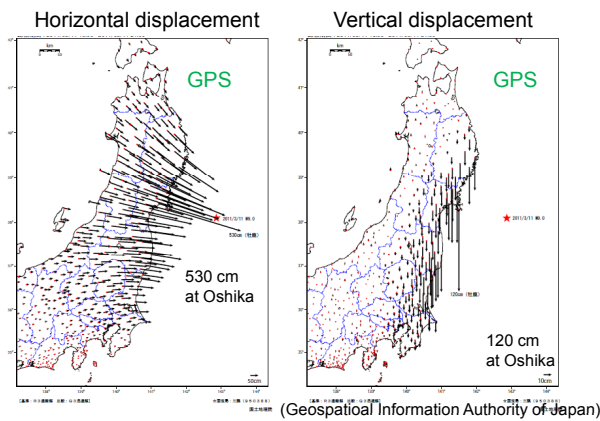


Figure 9: Subsidence due to coseismic slip (Fujita, 2011)

response can be assessed with the nonlinear finite element method with confidence, if however, the loading condition is known accurately.

11 ABNORMAL ENVIRONMENTAL ACTIONS

Abnormal waves have many times been reported in the maritime folklore, but until recently it was believed that these huge waves only existed in legends. These waves have been known under many different names such as: rogue waves, freak waves, killer waves, extreme waves and abnormal waves. In the following the term freak waves will be used.

11.1 *Freak Waves*

In oceanography freak waves are according to WIKIPEDIA (2010) defined as waves whose height is more than twice the significant wave, which is itself defined as the mean of the largest third of waves in a wave record. Therefore freak waves are not necessarily the biggest waves found at sea. They are rather, surprisingly large waves in a given sea state.

The existence of freak waves was not positively confirmed until New Year's Day 1995 at the Norwegian Draupner jacket platform, where an unusually large wave was recorded and analysed (Haver, 2004a). The wave record is shown in Figure 10.

A close examination showed that the wave crest was large, but not beyond the abnormal (10^{-4}) wave crest specified for the design. However, it was much higher than could be associated with the measured sea states. The crest height was well beyond the 10^{-2} crest height, but the platform loads did not exceed that level. This suggests that the shape of the wave differs from typical design waves. In Haver (2004b) it was found that freak waves should be considered a separate population well beyond the population used for design purposes. Further, it was found that freak waves are not seen as likely to represent a problem for offshore structures with the frequency of occurrence experienced so far. Nevertheless, to achieve robustness against unknown freak wave extremes it is in Haver (2004b) recommended to include an accidental (10^{-4}) wave event in the design process.

11.2 *Tsunami Waves*

Very little guidance is provided in currently available structural design codes, standards and guidelines on actions from tsunamis. However, in FEMA P646 (2008) important experience in relation to tsunamis and the design actions generated by tsunamis

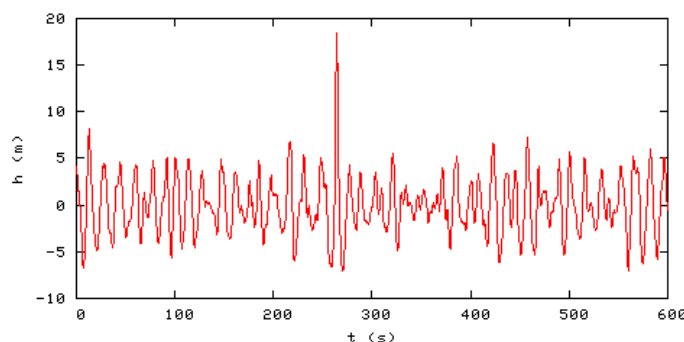


Figure 10: The Draupner wave, a single giant wave measured at New Year's Day 1995, finally confirmed the existence of freak waves, which had previously been considered near-mythical.

is discussed. Although FEMA P646 (2008) addresses the design of structures for vertical evacuation from tsunamis on the shore, the fundamental issues, namely how to predict design actions from tsunamis are shared with offshore structures.

Tsunamis are created in a variety of ways. Perhaps the best known generation mechanism is earthquake-induced displacement of the sea bottom, which causes a related sea-surface elevation that then propagates away from the generation area due to gravity. In case of the 3.11 disaster in Japan, the tsunami had a wave height of up to 25 m as a result of the earthquake. Additionally, submarine slumping of the offshore shelf or the impact of a terrestrial landslide into the sea can also cause devastating tsunami wave.

Similar to other hazards structural design criteria for tsunami effects should be based on the relative tsunami hazard, i.e. given a known or perceived tsunami threat in a region, the first step is to determine the severity of the tsunami hazard. This involves identification of potential tsunami generating sources and accumulation of recorded data on tsunami occurrence and run up. The assessment of tsunami hazard can include a probabilistic assessment considering all possible tsunami sources, or a deterministic assessment considering the maximum tsunami that can reasonably be expected to affect a site. Once potential tsunami sources are identified, and the level of tsunami hazard is known, site-specific information on the extent of inundation, height of run up, and velocity of flow is needed. Given the tsunami hazard and extent of inundation, the potential risk of damage, and loss of life must then be evaluated.

In FEMA P646 (2008), the design tsunami is termed the Maximum Considered Tsunami (MCT). It is anticipated that the hazard level corresponding to the Maximum Considered Tsunami will be consistent with the 2500-year return period associated with the Maximum Considered Earthquake used in seismic design.

For site-specific tsunami hazard assessment, the Maximum Considered Tsunami, should be developed using the Deterministic Maximum Considered Earthquake (Deterministic MCE) as the source (initial condition) of the tsunami model.

It should be noted that the above recommendations do not include modelling for tsunamis induced by landslides, volcanoes, or meteorite impacts.

There is significant uncertainty in the prediction of hydrodynamic characteristics of tsunamis because they are highly influenced by the tsunami waveform and the surrounding topography and bathymetry.

It is essential for the area of refuge to be located well above the maximum tsunami inundation level anticipated at the site. Determination of a suitable elevation for a tsunami refuge must therefore take into account the uncertainty inherent in estimation of the tsunami run up elevation, possible splash-up during impact of tsunami waves, and the anxiety level of evacuees seeking refuge in the structure. To account for this uncertainty, the magnitude of tsunami effects is determined assuming a maximum tsunami run up elevation that is 30 % higher than values predicted by numerical simulation modelling or obtained from tsunami inundation maps. It is further recommended that the refuge elevation include an additional 3 m allowance for freeboard above this elevation. The recommended minimum refuge elevation is therefore the anticipated tsunami run up plus 30 % plus 3 m.

Seismic loads are not considered to act in combination with tsunami loads. While aftershocks are likely to occur, the probability that an aftershock will be equivalent in size to the Maximum Considered Earthquake and will occur at the same time as the maximum tsunami inundation is considered to be low.

12 ICE AND ICEBERGS

The importance of marine transport in the Arctic Regions is further increasing as the ice-extends decrease. The latter, may also contribute to severe ice conditions with large drifting floes, ridges and icebergs as a result of calving or ice field separation combined with northern winds and currents. Therefore, structures need to be designed to withstand the local pressures and the resulting global impact. These structures, usually fixed and rarely floating can collide with drifting ice, ridges, crawlers or icebergs. As a result, their impact velocity is relatively low, however, neglecting a ship colliding with ice at service speed.

Several guidelines and regulations are concerned with brash ice conditions, e.g. a broken channel in level ice; see for example Finish-Swedish ice rules. However, only a limited number of regulations are dealing specifically with extreme loads.

ISO 19902 is concerned with the energy absorption during an iceberg impact arising from the combined effect of local and global deformation. The energy absorbed shall be compared with, and equated to, the impact (kinetic) energy due to a ship collision, and the results shall be documented. Before the publication of ISO 19906 on Arctic structures, all requirements for the design of structures for ice and iceberg loads shall be in accordance with CAN/CSA-S471-04. Furthermore, the design of stiffened plate panel configurations other than uniaxial stiffened plate panels shall be in accordance with other design standard such as DNV-RP-C201 or API Bulletin 2V.

The NORSOK standard N-003 8.3.2 concerns vessel collisions and should be followed according to 6.4.2.3 for iceberg collisions. Furthermore, 6.4.2.3 states the geographical location for iceberg collisions in the Barents Sea together with the probability of exceedance. Additionally, 8.3.2 states that all relevant traffic data needs to be collected for the site in question including icebergs. Hence, the most probable loading may be derived from this collection. Furthermore, a simplified supply ship impact scenario is described, which may be considered for an iceberg collision too. However, a design iceberg and scenario are yet missing a standardized load assessment.

Furthermore, new Polar class rules are about to be released, with eventually more details on such extreme ice impact. The likelihood of, i.e. iceberg impact, needs to be investigated for the site in question. Furthermore, one of the main challenges in iceberg collisions with ships and offshore structures is to obtain the correct magnitude of local pressure acting on the surface of the structure as a result of the ice impact. Recent studies involve full-scale measurements of the local ice pressure during the CCGS Terry Fox bergy bit impact, see Ritch *et al.* (2005) and Johnston *et al.* (2007). Local pressures of up to 10 MPa have been reported, but higher values may be probable too. Furthermore, Eik and Gudmestada (2010) found that the maximum impact load corresponding to a 10,000-year event was 85 MJ and that this value can be reduced to 1.8 MJ if an iceberg management system with iceberg detection, iceberg deflection and disconnection capabilities including emergency disconnect is used.

In this respect, commonly the existing standards fail to give a clear design guideline concerning iceberg collision and need to be improved. Furthermore, new ice material models should be developed to contribute to development of these guidelines; see also Chapter 16.

13 FLOODING

Accidental flooding is one of the main topics related to incidents connected with ships and offshore structures. The obvious major concerns are loss of buoyancy and stability.

Members of the International Towing Tank Conference have carried extensive research on this topic and are still continuing. A recent article by Santos (2009), starts with a nice introduction into the topic. A third issue related to flooding is structural loading, which seems to have attracted much less attention from researchers. Therefore Committee V.1 has decided to dedicate this chapter to this issue.

13.1 State-of-the-art

Very little literature is available on the effect of flooding on the structural integrity of a ship or a floating offshore structure. This may not be surprising because in most reported disasters where flooding played a role, usually (hydrostatic) stability is recognised as the main issue.

When a strength issue comes into play there are in principle two mechanisms;

1. The floodwater changes the ‘deadweight’ distribution along the ship’s hull girder to such an extent that still water bending or torsional moments exceed the capacity of the structure, or reduce the strength margin available for wave loads and loads due to inertia forces.
2. The motions of the floodwater cause pressure loads which exceed the capacity of the bulkheads of the flooded compartments.

Few publications are known to the committee which deal with hull girder loads due to flooding explicitly. Korkut *et al.* (2005) report model test results with a damaged ship ($L_{pp} = 173\text{ m}$) in regular waves. They demonstrate that hull girder loads may increase significantly under damaged condition, to such an extent that they should not be ignored. Figure 11 shows the increase of the torsional moment ‘RAO’ due to engine room flooding.

SSC report 445 does not confirm this finding, it actually states that for the ship investigated, a cruise liner with an $L_{pp} = 242\text{ m}$, bending moments tend to decrease in damaged condition. However, this may be caused by the way in which the analyses were made, where bending moments were calculated through an equivalent design wave, based on predicted wave bending moments with the Ship Motion Program software from David Taylor Model Basin.

It is convenient to refer to the flood water pressure load mechanism as sloshing loads. Gao *et al.* (2011), report on an extensive research effort on the numerical simulation of flooding. The paper includes flood water load predictions on bulkheads which compared favourably with results from model scale tests on a barge. Another interesting

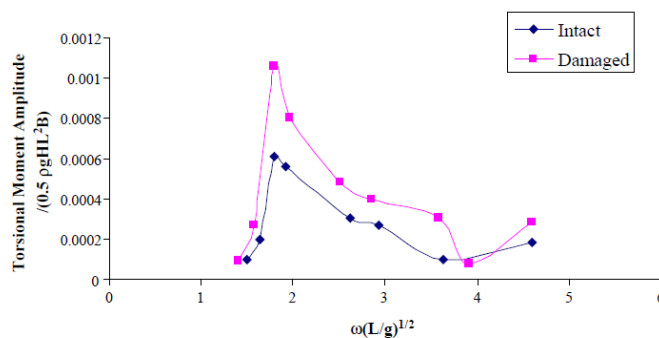


Figure 11: Comparisons of torsional moment R.A.Os at mid-ship in beam seas for large wave height (Korkut *et. al.*, 2005).

article is from Le Touzé *et al.* (2010), who report on the use of Smoothed Particle Hydrodynamics (SPH) for predicting green water and flooding phenomena, which compare favourably with test results. Loads due to flooding are not included in the reported study. However, an article by Dolorme *et al.* (2005), also describes the use of SPH, but now related to sloshing. Satisfactory results are reported with respect to predicted loads on bulkheads.

Ming *et al.* (2010), report on sloshing load prediction methods based on the Volume Of Fluid method. The method is validated against test data recommended by the 23rd ITTC Committee as a benchmark case.

13.2 *Suggestions for further Research*

Availability of well documented sloshing test data, including the geometry of the inner tank structure, tends to be limited. The committee suggests including data collected by SSC on this topic (SSC report 336) in validations.

It is also suggested to extend efforts on research related to global internal loads of floating structures while flooded, including sloshing resonance while in sea states.

14 ILLEGAL ACTIVITIES LIKE USE OF EXPLOSIVES AND PROJECTILES

It is projected that world consumption of marketed energy is to increase by 49% from 2007 to 2035 (EIA, 2010). This dependency will grow inexorably as the populace in developing countries replace the use of traditional fuels with marketed ones, such as propane and electricity. Most of the estimated remaining energy reserves are located offshore politically unstable nations, while new explorations take place in areas of long-term assertions (Barents Sea, Aegean Sea, Libyan Sea). During the Iraq-Iran war (1980-1988) several oil fields were attacked and damaged significantly. The Dorra Field is a characteristic example where platforms were attacked indiscriminately during the conflict.

14.1 *Terrorist Attack Assessment and Consequences*

According to the RAND Corporation's terrorism database only 2% of all terrorist incidents since 1969 are conducted in the marine environment. Some examples of terrorist attacks on offshore vessels are shown in Figure 12. In these cases most attacks resulted in severe damage to the target structures. The M Star tanker had significant hull deformation, as shown in Figure 12(a), the MV Limburg, Figure 12(b), USS Cole Figure 12(c), had large holes blown in the side of the vessels and Superferry 14, Figure 12(d), sunk as a result of the explosions.

The costs and environmental effects associated with structure damage due to a terrorist attack can be significant, in the case of the MV Limburg, 90,000 barrels of oil leaked into the Gulf of Aden.

Although terrorist attacks have historically been carried out with the use of explosives, this does not preclude future threats from the use of missiles, ramming with large vessels, or use of divers or unmanned underwater vehicles from planting or detonating underwater charges. The structural assessment and load definitions due to a terrorist event could fall into several categories that have been detailed throughout this report including hydrocarbon explosions and fires, underwater explosions, ship impacts and flooding.

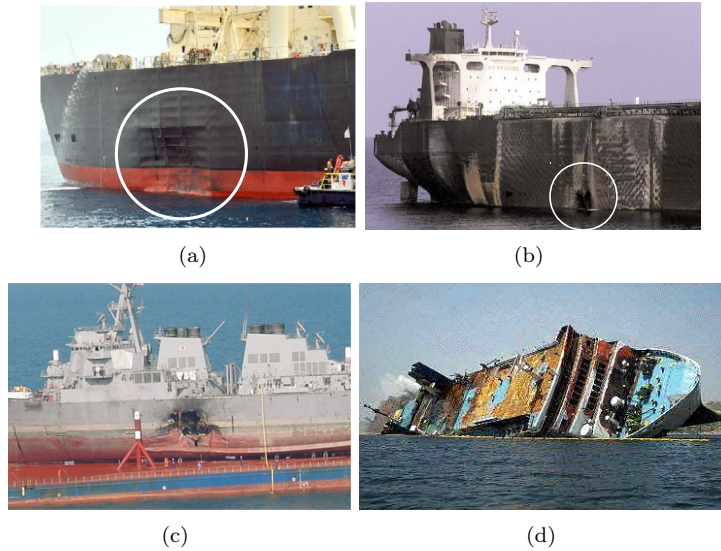


Figure 12: Consequences of historical terrorist attacks on offshore structures (a) M Star tanker, (b) MV Limburg supertanker, (c) USS Cole warship, and (d) Superferry 14

14.2 Definition of Loads

An intentional explosion onboard an offshore platform may result from a relatively small incendiary device after an intended gas leak or an improvised explosive device (IED) planted either above or below the water. Standoff weapons can also be used from a distance outside the facility giving terrorists a safe vantage distance.

Rocket-propelled grenades (RPG) are widely sold in every corner of the world nowadays. It is estimated that as of 2002, at least 9 million RPGs had been produced around the world (O'Sullivan, 2002). RPGs' light weight, low acquisition cost, ruggedness, and reusability are some of the key reasons that make them a weapon of choice with some militia and irregular forces in Southeast Asia and the Middle East (Grau, 1998). RPGs are capable of penetrating up to 500 mm of steel. There is no doubt that their jet can penetrate thin plates used in marine and offshore structures. Figure 13 shows the ballistic response of a cross stiffened panel upon impact with an RPG. The shaped charge jet effortlessly penetrates the panel causing an insignificant out-of-plane displacement in the target.

Figure 14 depicts the out-of-plane deformation of a 10 mm witness plate impacted by a scaffold clip at 150 m/s. Although the plate does not perforate, the kinetic energy of the projectile could inflict lethal injuries on personnel. In a similar manner tools, pipes, fire extinguishers and other loose objects can be turned into projectiles with grave consequences.

Another popular modus operandi is that of explosively-laden skiffs or zodiacs that detonate alongside their target (USS Cole type of attack). The riser as well as tubular members of the facility at the waterline can be damaged in this manner leading to possible fire and or environmental damage or loss of the platform. Figure 15 and Figure 16 depict damage inflicted to a riser and typical offshore joint from a detonation at sea level.

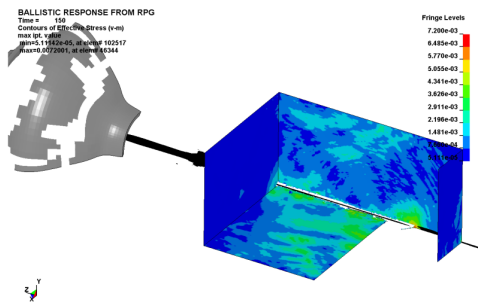


Figure 13: FE prediction of equivalent stresses (Mbar) in the target panel (Pahos, 2011)

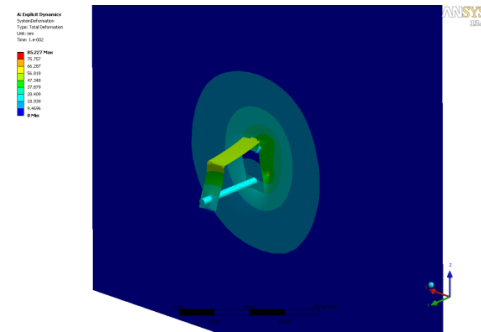


Figure 14: Deformation of witness plate from impact of a scaffold clip

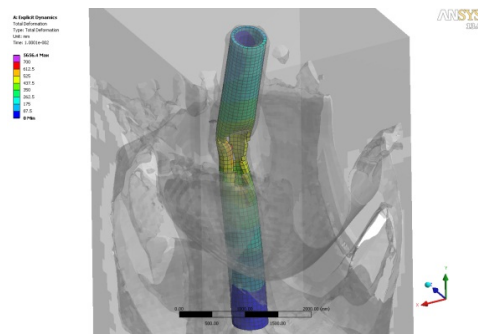


Figure 15: Structural response of a riser from detonation at sea level

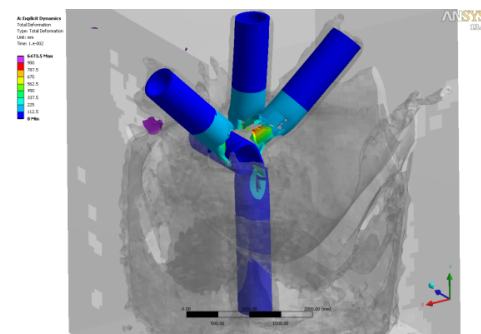


Figure 16: Structural response of a typical joint commonly encountered in offshore structures

Careful placement of numerous charges at critical locations could cripple the structural members. In addition, blast waves can be focused and amplified with different geometries and initiation points (Carl and Pontius, 2006).

15 DESIGN AND ASSESSMENT PROCESS

The design and assessment process is a part of the total safety management of offshore installations. In Moan (2007) an overview of important developments regarding safety management of offshore structures is given. It is found that the risk can be controlled by the use of adequate design criteria, inspection, repair and maintenance of the structure as well as quality assurance and control of the engineering processes.

By experience, it is often human errors that initiate catastrophic accidents. Damage tolerance is therefore seen as a desirable feature of a structure. Moan (2007) demonstrated how an acceptable risk level may be achieved by introducing Accidental Collapse Limit State (ALS) criteria in the design of offshore structures.

The new ISO standards for offshore structures, see e.g. ISO 19902 (2007), offer a practical implementation of the design approach against accidental or abnormal actions through the identification of relevant hazards and subsequent design using ALS criteria, in principle as proposed in Moan (2007).

15.1 Codes and Standards

15.1.1 General

The focus on Accidental Collapse Limit State (ALS) criteria in the design requirements in different design standards has increased over the last 10-15 years especially for structures of high importance. Irrespective of this development, different approaches both in complexity and completeness are currently used in different design standards. Within the offshore industry the most important sources are Norsok N-004 (NORSOK, 2004), and ISO (ISO 19902, 2007), and the text in this chapter is largely reflecting these criteria.

15.1.2 Robustness

In the new ISO standards for offshore structures it is required that damage from events with reasonable likelihood of occurrence shall not lead to complete loss of integrity of the structure. Further, it is emphasized that the structural integrity in the damaged state shall be sufficient to allow for process system close down and a safe evacuation.

In ISO 19902, (ISO 19902, 2007), it is specifically stated (Clause 7.9) that: 'A structure shall incorporate robustness through consideration of the effects of all hazards and their probabilities of occurrence, to ensure that consequent damage is not disproportionate to the cause'.

The robustness concept is therefore closely related to accidental actions and abnormal actions, consequences of human error and failure of equipment. In ISO terminology such situations are denoted 'hazardous circumstances' or briefly 'hazards'.

Robustness is achieved by considering accidental limit states (ALS) that represent the structural effects of hazards. Ideally all such hazards should be identified and quantified by means of a risk analysis, but in many cases it is possible to identify and quantify the most important hazards based on experience and engineering judgement.

15.1.3 Accidental Limit States

Accidental situations relate to two types of hazards:

1. *Hazards associated with identified accidental events*, often those from ship impact, dropped objects, fires and explosions.
2. *Hazards associated with abnormal environmental actions*, typically environmental actions with a return period of the order of 10,000 years.

The two types of hazards are different by nature. In principle accidental events can in some cases be avoided by taking appropriate measures to eliminate the source of the event or by bypassing and overcoming its structural effects. In contrast to this, the possible occurrence of abnormal actions cannot be influenced by taking such measures.

An accidental design situation is considered in an accidental limit state (ALS), and normally comprises the occurrence of an identified accidental event or abnormal environmental actions, in combination with expected concurrent operating conditions and associated permanent and variable actions.

15.1.4 Designing for Hazards

When the hazard cannot reliably be avoided, the designer has a choice between minimizing the consequences (the consequences of damaging or losing a structural component due to the hazard), or designing for the hazard (making the component strong enough to resist the hazard). In the first case, the structure should be designed in such a way that all structural components that can be exposed to a hazard are non-critical,

i.e. can be lost without causing failure of the whole structure or a significant part of it. In the second case, critical components that can be exposed to hazards (failure of which would cause failure of the whole structure or a significant part of it) shall be made strong enough to resist the hazard considered.

It is specifically noted in ISO 19902 that the robustness requirements do not imply that structures shall be able to survive removal of any structural component. If there is no hazard, then there is no requirement in relation to robustness. Also, only one hazard at a time should be considered.

15.2 Risk Assessment Issues

15.2.1 General

This chapter reviews and discusses the framework for a risk-based design against accidental actions in a broader perspective. Conceptually, the main elements in such a discussion are: the probability of a given accidental action, the conditional probability of damage given the accidental action and finally the conditional probability of a global failure given damage. In the following chapter these aspects will be discussed in some detail.

15.2.2 Accidental and Abnormal Actions

In Figure 17 taken from Moan (2007) accident rates for mobile (drilling) and fixed (production) platforms have been shown according to the initiating event of the accident. Although the curve is rather old, the general trend is still believed to be true. It is most noticeable that none of these accidents should occur, but they still do so because of operational errors and omissions. Despite the efforts made to avoid error induced accidental actions they cannot be completely eliminated. Therefore, Accidental collapse Limit State (ALS) criteria are introduced to prevent progressive failure.

In a rational ALS criterion the accidental action should be defined as a characteristic value preferably defined in probabilistic terms. This has been done both in ISO 19902 (ISO 19902, 2007) and Norsok (NORSOK, 2004) where the characteristic accidental action for offshore structures is specified by an annual exceedance probability of 10^{-4} .

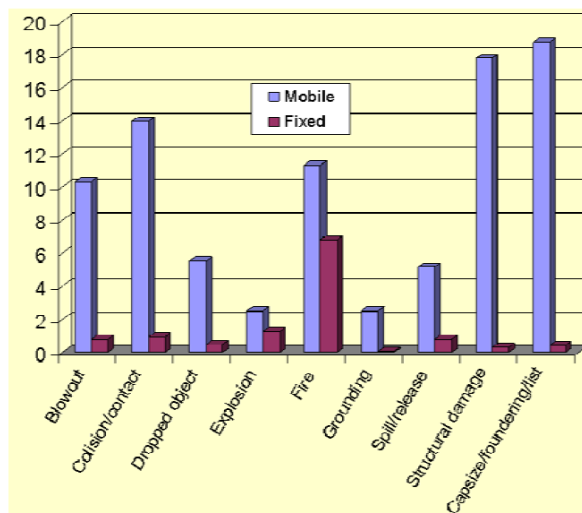


Figure 17: Number of accidents per 1000 platform-year

$$P_{FSYS}(i) = \sum_{j,k} P[FSYS | D] \cdot P[D | A_{jk}^{(i)}] \cdot P[A_{jk}^{(i)}]$$

probability of damaged system failure under relevant F&E actions
 probability of accidental action at location (j) and intensity (k)
 For each type of accidental action probability of damage, D given $A_{jk}^{(i)}$ (decreased by designing against large $A_{jk}^{(i)}$)
 $P[A_{jk}^{(i)}]$ is determined by risk analysis while the other probabilities are determined by structural reliability analysis.
 $P[FSYS | D]$ is determined by due consideration of relevant action and their correlation with the hazard causing the damage

Figure 18: Probability of system loss due to accidental action (i)

The ALS criterion also applies to abnormal environmental conditions such as hazards associated with abnormal environmental wave actions. In this connection focus should also be given to abnormal waves with high crest or unusual shape – especially in such cases where the 10^{-2} wave might not reach the platform deck, but the 10^{-4} wave crest hits the deck and causes a significant increase in the wave loading.

15.2.3 Framework for the Design Against Accidental Actions

As outlined in Moan (2007) a truly risk based design should account for the various sequences of progressive development of accidents into total losses. However, in a design context simplifications are necessary. One such approach is, as previously discussed, to prevent escalation of damage induced by accidental actions by requiring the structure to resist relevant actions after it was damaged.

The probability of system loss due to accidental action (i) may be written as shown in Figure 18 and to demonstrate compliance with ALS requirements calculation of damage due to the accidental actions is needed. In general nonlinear analysis is required to estimate structural damage, i.e. permanent deformation, rupture etc. of structure components.

According to Moan (2007) the implied conditional annual probability of failure for a damaged structure designed to Norsok criteria will be of the order of 0.1. The probability of total loss implied by the ALS criterion for each category of accidental or abnormal action would then be of the order of 10^{-5} .

As a further consideration in Moan (2007) it is mentioned that hazards associated with normal variability and uncertainty inherent in prescribed payloads and environmental loads and resistance are handled by ULS and FLS design criteria. Such criteria do not reflect human errors and the notional annual failure probability of components implied by current ULS requirements for offshore structures is of the order $10^{-3} - 10^{-5}$. Fatigue and fracture are controlled by a combination of design for adequate fatigue life and robustness (ALS criterion) as well as by inspection and repair. If the fatigue design factor is taken to be 1, the fatigue failure probability in the service life is 0.1, but this value can be reduced significantly by using more restrictive design criteria and/or inspection.

15.3 Assessment of Structural Consequences of Accidents

15.3.1 Numerical and Simulation Tools

Numerical modelling can be carried out with the use of various methods and types of solvers including finite element, computational fluid dynamics, and hydrocodes.

Table 7: Tools for Determining Accidental Actions

Code	Type of Code	Uses for load and consequence determination
ANSYS FLUENT Chinook Cobalt Kameneon FireEx FLACS	CFD	Fluid flow physics models Air and Underwater blast analysis software Detailed flow field diagnostics HC Fire loads HC Explosion loads
MSC/DYTRAN Abaqus/Explicit LS-DYNA	Explicit FE	Extreme short duration events Nonlinear continuum, transient dynamic phenomena Thermal, ALE, fluid-structure interaction, multi-physics coupling
ALE3D	FV and FE	Heat conduction, multi-phase flow, chemical kinetics, species diffusion, detonation, deflagration, convective burn

Various numerical and simulation tools are available and should be selected based on the event being modelled. Commercially available numerical analysis codes which can be used to predict the load and structural response resulting from accidental events are given in Table 7.

In many cases hydrocodes are within government or defence organizations and are kept proprietary.

15.3.2 Experimental Methods

In some cases experimental programs are required to determine the structural integrity due to accidental events, and can be used to validate numerical approaches. Experimental programs are generally carried out to determine the effects of air and underwater blast, dropped objects, and fire as well as determining nonlinear material properties. Due to costs, structure availability, and environmental effects experimental programs may be limited to smaller scale. Even though the costs are high, large scale experiments are very useful for verifying structural behaviour under extreme actions.

16 RESIDUAL STRENGTH/STRUCTURAL INTEGRITY

In most design standards it is a requirement that an after damage situation following an accidental event or abnormal environmental action shall be considered, and that the structure in this condition shall remain intact for a period of time sufficient for all personnel to be safely evacuated and all process equipment to be closed down to avoid pollution.

16.1 Damage Tolerance

For the design of new structures, or assessment of existing structures not triggered by actual damage, damage tolerance considerations must be based on accidental limit states reflecting the relevant hazards. If a linear structural analysis of the damage scenario indicates sufficient capacity of all components it is often assumed that the hazard has not damaged the structure, i.e. the resistance is not degraded in relation to the after damage situation. However, in most cases the structure's resistance is more or less reduced as compared to its undamaged condition, and a reliable prediction of the extent of the damage requires the application of non-linear structural analysis methods.

Different design standards tend to specify slightly different acceptance criteria for the after damage situation. In lieu of more specific requirements ISO 19902 requires the after damage situation analysed using environmental conditions with a return period of the order twice a conservative estimate of the time required to perform suitable repairs by which the structure's strength would be restored to the design strength, the minimum return period shall be one year. The strength of damaged components shall either be estimated using a rational approach (according to ISO 19902) or shall be neglected, and the normal design requirements (using the usual action and resistance factors) for the design of new structures apply.

16.2 Damaged Structures

For existing structures where physical damage has been detected, the nature and extent of the actual structural damage must be established.

The analysis of the damaged structure determines any immediate requirement for shut-in and/or evacuation as well as the need for temporary repairs, while awaiting a decision and plan for the implementation of definite repairs or abandonment. Verifications of the after damage design situation for physically damaged structures are typically carried out in compliance with the design requirements for assessment of existing structures. In some design standards the assessment criteria and the design criteria for new structures are identical, while e.g. ISO 19902 potentially allows the use of relaxed acceptance criteria (Clause 24).

16.3 Mitigation and Repairs

As discussed in Chapter 15.3.2 accidents, human and operational errors are the most important causes to failures of offshore structures. It is therefore primarily important to avoid these errors in order to limit the risk of undesirable events. Secondly, it is crucial to carry out quality assurance and control in all life cycle phases.

In Moan (2007) the causes of failures are categorized and the corresponding measures to control the accident potential are listed. In general the measures include design criteria, quality assurance and control (QA/QC) relating to the engineering process, as well as the hardware and operational procedures.

17 MATERIAL MODELS FOR STRUCTURAL ANALYSIS

Offshore structures exposed to hazards as defined above may undergo highly non-linear structural deformations, including rupture. Therefore, finite element analyses of these events require the input of appropriate material relations including failure representing the local material behaviour. Depending on the hazard to be analysed and the materials found on the offshore structures a selection of recommended material models can be made, see Table 8. The physical origin of these material models will be briefly presented, followed by numerical implementation possibilities as well as comments, hints and shortcomings arising from the use of those models as well as concerns of guidelines and standards. However, hazard simulations utilizing the recommended material models and input parameters can be used for basic physical checks, but they may not be applicable in general.

The material modelling represents a crucial part of all numerical simulations, because it predefines how the material is assumed to behave during the simulations. Hence, the ability of the material model to represent the physical behaviour accurately directly influences the accuracy of the simulation results and their reliability. Furthermore,

Table 8: Recommended material models and associated hazards.

Hazard	Material										
	Steel	Aluminium	Foam, Isolator, Rubber	Ice	Air	Water	Explosives	Risers, umbilical or power cables	Composite	Concrete	Seabed
Hydrocarbon explosions	■	■	■					■	■	■	
Hydrocarbon fires	■	■	■					■	■	■	
Underwater explosions	■	■	◆		■	■	■		◆	◆	◆
Wave Impact	■	■	■			■		◆	■		
Water-In-Deck	■	■	■			■			■		
Dropped Objects	■	■	■			◆		◆	■	■	■
Ship Impact	■	■	■	■				◆	■	■	◆
Earthquakes	■	■	■			◆		■	■	■	■
Ice, Iceberg	■	■		■		■		■	■	■	
Flooding	■	■	■		■	■			■		

■ - recommended, ◆ - recommended where applicable

the correct physical behaviour may be represented well by the underlying assumptions of the material model, because it can correspond well to the physical experiment done to obtain the properties of the material in question. However, whether or not this experiment or the correspondence represents the true material behaviour remains often a question, e.g. a classical tensile experiment is a material test by agreement even though a structural test is carried out. Hence, the utilization of such experimentally based material models using small structural tests can lead to inconsistent results when applied to general structures. Furthermore, it remains often questionable whether the obtained material model corresponds to the discrete mathematical model, i.e. the finite element mesh, of the structure to be analysed. Hence, a material model should be unique and usable for any mesh size or conditions and should therefore not affect the results with a change in discretization of the simulation domain. In the past, often the term ‘true’ material model was utilized, which is however misleading as it implies that it is ‘true’ by all means and could be universally applied. In fact, all material measures are ‘true’ with respect to their determination scale, i.e. the engineering measure obtained by a tensile experiment is true with respect to the specimens’ gauge length.

Hence, this chapter seeks to provide appropriate guidance to identify the material model to be used with the associated hazard according to Table 8 in such a way that it is consistent with the discretized, respectively meshed, simulation domain. Furthermore, engineering based best practices are provided as well as the associated shortcomings. The nomenclature of the numerical implementation used in the material input cards can be found in Hallquist (2007). The effects the material models account for, e.g. strain rate, temperature or damage criteria, will be provided alongside a selection of references relevant to the given material. Thereby, this database of material models will clarify common questions and uncertainties associated with the use of material models.

17.1 Guidelines and Standards

ISO 19902 Ed. 1 requires that the expected non-linear effects, including material yielding, buckling of structural components and pile failures, should be adequately modelled and captured. Strain rate effects should be considered as well as temperature dependency. NORSOK standard N-003 and DNV Recommended Practices DNV-RP-C204 suggest the use of the temperature dependent stress-strain relationships given in NS-ENV 1993 1-1, Part 1.2, Section 3.2. To account for the effect of residual stresses

and lateral distortions compressive members should be modelled with an initial, sinusoidal imperfection with given amplitudes for elastic-perfectly plastic material and elasto-plastic material models. General class rules or CSR commonly state that an appropriate material model should be used; possibly in the form of a standard power law based material relation for large deformation analysis of steel structures. Additionally, some specify critical strain values to be used independent of the mesh size, which should, however, be sufficient, may be specified.

Hence, these guidelines and standards fail to provide a clear guidance for the analyst and may easily lead to diverse results simply by choosing different, yet not necessarily physically correct, material parameters.

17.2 Material Model Database

17.2.1 Steel

Commonly, the nonlinear material behaviour is selected in the form of a power law; see, for example, Alsos *et al.* 2009 and Ehlers *et al.* (2008). The power law parameters can be obtained from standard tensile experiments; see Paik (2007). However, with this approach agreement between the numerical simulation and the tensile experiment can only be achieved by an iterative procedure for a selected element size chosen a priori. Hence, the procedure needs to be repeated if the element size is changed.

Furthermore, the determination of the material relation alone does not necessarily suffice, as the failure strain, i.e. the end point of the stress versus strain curve, depends in turn on the material relation. However, a significant amount of research has been conducted to describe criteria to determine the failure strain, for example by Törnqvist (2004), Scharrer *et al.* (2002), Alsos *et al.* (2008), and to present their applicability (e.g. Tabri *et al.* 2007 or Alsos *et al.* 2009). However, all of these papers use a standard or modified power law to describe the material behaviour, and none of these papers identifies a clear relation between the local strain and stress relation and the element length.

Relations to obtain an element length-dependent failure strain value are given by Peschmann (2001), Scharrer *et al.* (2002), Törnqvist (2004), Alsos *et al.* (2008) and Hogström *et al.* (2009). These curve-fitting relations, known as Barba's relations, are obtained on the basis of experimental measurements. However, they define only the end point of the standard or modified power law. Hence, Ehlers *et al.* (2008) conclude that the choice of an element length-dependent failure strain does not suffice in its present form.

Therefore, Ehlers and Varsta (2009) and Ehlers (2009a) presented a novel procedure to obtain the strain and stress relation of the materials, including failure with respect to the choice of element size using optical measurements. They introduced the strain reference length, which is a function of the discrete pixel recordings from the optical measurements and corresponds to the finite element length. As a result, they present an element length dependent material relation for NVA grade steel including failure, see Figure 19.

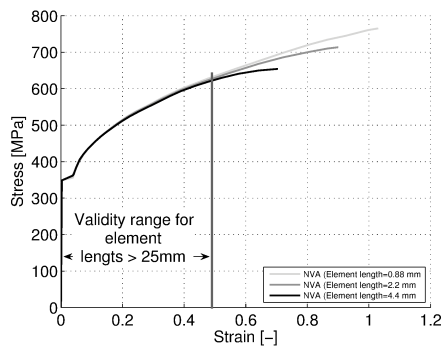
Moreover, Ehlers *et al.* (2010) identified that a constant strain failure criterion suffices for crashworthiness simulations of ship structures and that the strain rate sensitivity of the failure strain and ultimate tensile force is less than three per cent, see Figure 20. Hence, for moderate displacement speeds the strain rate influence is negligible.

An example input card following the LS-DYNA nomenclature for a piece-wise linear material (mat.24) is given in Table 9.

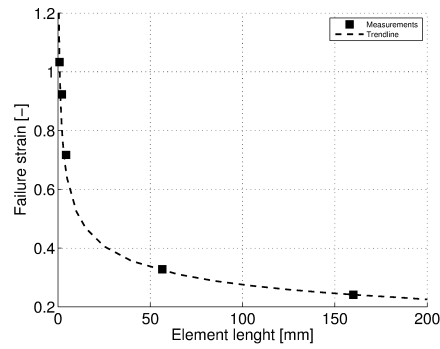
Table 9: Piece-wise linear steel material model

```

*MAT_PIECEWISE_LINEAR_PLASTICITY
$# mid ro e pr sigy etan fail tdel
$# 1 7850.00 2.06E+11 0.3000 3.423E+8 0.000 0.661000 0.000
$# c p lcss lcsr vp
$# 0.000 0.000
$# eps1 eps2 eps3 eps4 eps5 eps6 eps7 eps8
$# 0.006 0.02612 0.04019 0.06865 0.15071 0.345 0.64477 0.74
$# es1 es2 es3 es4 es5 es6 es7 es8
$# 3.423E+8 3.530E+8 3.731E+8 4.219E+8 4.901E+8 5.827E+8 6.621E+8 6.737E+8
    
```



(a)



(b)

Figure 19: NVA grade steel: measured local strain and stress relation (a) and failure strain (b) (Ehlers 2009b)

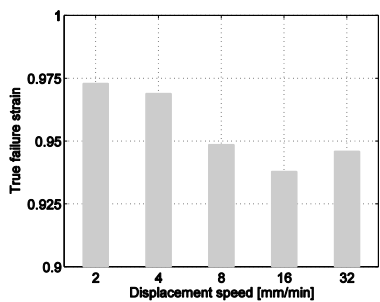


Figure 20: Deformation of witness plate from impact of a scaffold clip

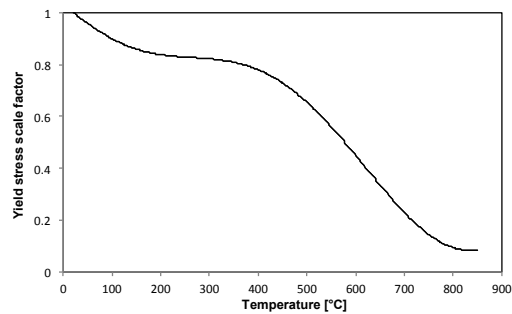


Figure 21: Global yield stress scale factor versus temperature for mild steel

However, the material behaviour, that is the change in the yield stress, at higher strain rates, $\bar{\epsilon}$, can be calculated according to the Cowper-Symonds relation

$$1 + \left(\frac{\bar{\epsilon}}{C}\right)^{1/p}$$

where C , p are the strain rate parameters and may be chosen as 40.4/sec and 5 for mild steel, respectively. Additionally, effects on elevated temperatures may be accounted for by scaling the global yield stress as a function of the temperature, see Figure 21.

The increase in yield- and ultimate strength at cryogenic temperatures, i.e. -100 and -163°C , is presented by Yoo *et al.* (2011) for mild stainless steel.

17.2.2 Aluminium

Various thin-walled aluminium structures under crash behaviour, i.e. large deformations including rupture, have been analysed experimentally and numerically in the past.

Langseth *et al.* (1998) uses an elasto-plastic material model with isotropic plasticity following the von Mises yield criterion and associated flow rule, see Berstad *et al.* (1994). Strain rate effects are often neglected for aluminium alloys, such as AA6060, in the strain rate range of 10^4 to 10^3 s^{-1} , see for example Lindholm *et al.* (1971). As a result, Langseth *et al.* are able to obtain good correspondence in terms of deformed shape, and shape of the force-displacement curve.

However, if high strain rates are to be expected, then the yield stress scaling according to Cowper-Symonds may be used. Négre *et al.* (2004) study the crack extension in aluminium welds using the Gurson-Tvergaard-Needleman (GTN) model and obtain reasonable correspondence in terms of force versus crack mouth opening displacement (CMOD). However, the GTN model requires a vast amount of input parameters whose physical origin cannot be directly provided. Furthermore, Négre *et al.* use 8-node brick elements, which are not suitable for large complex structures at present. Hence, from an engineering viewpoint this model does not suffice.

Lademo *et al.* (2005) utilize a coupled model of elasto-plasticity and ductile damage based on Lemaitre (1992) using the critical damage as an erosion criterion. They are able to simulate aluminium tensile experiments numerically with very good agreement using co-rotational shell elements and an anisotropic yield criterion Yld96 proposed by Barlat *et al.* (1997).

Such advanced material models can be easily implemented into numerical codes, and further increase in yield and ultimate strength at cryogenic temperatures, i.e. -100 and -163°C , can be considered following the results by Yoo *et al.* (2011) for mild aluminium. Furthermore, a strain reference length-based approach using optical measurements as proposed by Ehlers (2009a) for steel may be used to obtain a consistent material relationship. However, for most analyses a consistent determination of the global material behaviour, see Figure 22, together with a von Mises yield criterion will suffice.

An example input card following the LS-DYNA nomenclature for a piece-wise linear material (mat.24) is given in Table 10.

Table 10: Piece-wise linear aluminium material model

```
*MAT_PIECEWISE_LINEAR_PLASTICITY
$# mid ro e pr sigy etan fail tdel
    1 2.712E-9 75499 0.3000 200 0.000 0.1063 0.000
$# c p lcsc lcsr vp
    0.000 0.000
$# eps1 eps2 eps3 eps4 eps5 eps6 eps7 eps8
    4.940E-4 8.928E-4 0.002087 0.01000 0.03630 0.0796
$# es1 es2 es3 es4 es5 es6 es7 es8
    220.7480 230.8739 241.2000 253.2500 270.3999 293.2200
```

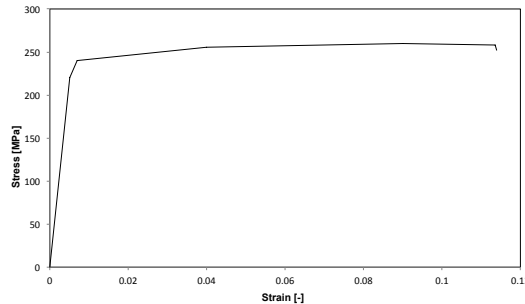


Figure 22: Example of a global strain versus stress curve from experiments

17.2.3 Foam, Isolator, Rubber

Gielen (2008) presents an isotropic polyvinyl chloride (PVC) foam model, which exhibits elasto-damage behaviour under tension and elasto-plastic behaviour under compression. His damage model is consistent with the physical behaviour of the foam, a full-scale application and verification is however missing.

Cui *et al.* (2009) present a model for uniform foam based on Schraad and Harlow (2006) for disordered cellular materials under uni-axial compression. As a result, they obtain various influencing parameters affecting the energy absorption capacity under impact. Hence, functionally graded foams may be used to increase impact resistance.

In the case of rubber, a simplified rubber/foam material model (mat_181) may be used, which is defined by a single uni-axial load curve or by a family of uni-axial curves at discrete strain rates, see Figure 23. An example input card following the LS-DYNA nomenclature for such rubber material is given in Table 11.

Table 11: Simplified rubber/foam material model

```

*MAT_SIMPLIFIED_RUBBER/FOAM
$# mid ro k mu g sigf ref prten
1 1.75E-9 1000 0 0 0 0 0
$# sgl sw st lc/tbid tension eps6 avgopt pr/beta
80 50 15 1 0 0 0 0.495
    
```

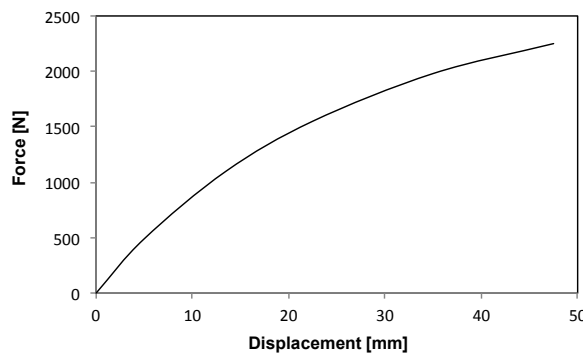


Figure 23: Exemplary force-displacement curve for rubber referenced as LC/TBID in mat_181

Table 12: Simplified ice material model

```

*MAT_ISOTROPIC_ELASTIC_FAILURE
$#      mid      ro      g      sigy      etan      bulk
      1  916.96000  3.0800E+9  7.6000E+5  6.8900E+9  8.0300E+9
$#      epf      prf      rem      trem
      0.010800  -3.080E+5      0.000      0.000

```

17.2.4 Ice

One of the main difficulties when modelling ice is the prediction of ice failure, i.e. fracture, under loading at temperatures around the melting point of the ice. Thus the local ice-structure interaction includes transitions between the different phases. The failure process of ice begins when the edge of the moving ice hits the structure. This contact induces loads to the edge of the ice causing a stress state in the ice. When the stresses exceed the strength of ice, it fails. Ice becomes ductile with visco-elastic deformations during low loading rates and brittle during high loading rates.

Polojärvi and Tuhkuri (2009) developed specialized simulations tools utilizing the boundary element method, whereas Forsberg *et al.* (2010) utilize the cohesive element method (CEM) to model ice failure. The latter is however of highly stochastic, or even random, nature and eventually results in reasonable agreement if experimental validation data becomes available.

However, Liu *et al.* (2010) treat the ice in a coupled dynamic ship – iceberg collision as an isotropic material, see Riska (1987), using the well-known Tsai-Wu strength criterion, see Tsai (1971). As a result, the obtained numerical results give an indication of the structural damage of the ship structure. However, their model erodes the ice at failure in an unphysical fashion resulting in purely numerical pressure fluctuation in the contact surface.

Therefore, the underlying material models and ice properties are in need to be defined consistently to account for the possible scatter and thereby to result in reliable design methods for ships and offshore structures. Hence, unless material model data is not available explicitly for tension and compression including an appropriate failure criterion for brittle ice failure based on micro-crack growth, a simple elastic model may be employed. The latter is however only valid to some extent, if, e.g. the flexural strength of an ice sheet is of interest.

Therefore, as a first attempt, ice may be modelled as a volumetric body following non-iterative plasticity with a simple plastic strain failure model (mat_13). However, therein the yield- and failure stress is not rate or pressure dependent and the temperature is assumed constant. An example input card following the LS-DYNA nomenclature for Baltic Sea ice is given in Table 12.

17.2.5 Air

For numerical simulations of structures subjected to underwater explosions, where the target is air-backed, the air needs to be modelled. The main material parameters are the mass density and the equation of state (EOS). The latter can be expressed

Table 13: Air material model

```

*MAT_NULL (n, kg)
$#      mid      ro      pc      mu      terod      cerod      ym      pr
      1      1.280      0.000      0.000      0.000      0.000      0.000      0.000

```

Table 14: Linear polynomial equation of state for air

```

*EOS_LINEAR_POLYNOMIAL (cm, g)
$# eosid      c0      c1      c2      c3      c4      c5      c6
      1      0.000    1.0e-02    0.000    0.000    0.400    0.400    0.000
$#   e0      v0
      0.000    0.000
*END

```

Table 15: Ideal gas equation of state for air

```

*EOS_IDEAL_GAS
$# eosid      cv0      cp0      c1      cq      t0      v0
      1 718.0000 1005.000    0.000    0.000    270.00    1.000

```

as a linear polynomial defining the pressure in the gas as a linear relationship with the internal energy per initial volume. The ideal gas EOS is an alternative approach to the linear polynomial EOS with a slightly improved energy accounting algorithm. In most cases, the mass density is the only parameter defined for the air. The same material properties were used in Trevino (2000) and Webster (2007).

An example input card for air following the LS-DYNA nomenclature is given in Table 13 according to Webster (2007).

The EOS example input following the LS-DYNA nomenclature is given in Table 14 according to Webster (2007) in the most common form, which defines the parameters such that it is an ideal gas behaviour.

Do (2009) describes the calculation process of e_0 , which can be used to define an initial pressure within the air. Additionally, an example input card for the ideal gas EOS following the LS-DYNA nomenclature is given in Table 15 according to Marc Ltd. (2007).

The ideal gas EOS is the equivalent of the linear polynomial with the C_4 and C_5 constants set to a value of $(\gamma - 1)$.

17.2.6 Water

When conducting simulations of structures subjected to underwater explosions, water models are required.

The primary mechanical property to be defined is the mass density and in some cases the pressure cut-off and dynamic viscosity coefficient is needed. The cut-off pressure is defined to allow the material to numerically cavitate when under tensile loading. This is usually defined as a very small negative number, which allows the material to cavitate once the pressure goes below this value.

Table 16: Material model for water (Trevino, 2000)

```

*MAT_NULL (cm, g)
$# mid      ro      pc      mu      terod      cerod      ym      pr
      1 1.000000    0.000    0.000    0.000    0.000    0.000    0.000

```

Table 17: Material model for water (Webster, 2007)

```

*MAT_NULL (m, kg)
$# mid      ro      pc      mu      terod      cerod      ym      pr
      1 1025.000 -1.0e-20  1.13e-3    0.000    0.000    0.000    0.000

```

Table 18: Equation of state for water

```
*EOS_GRUNEISEN
$# eosid      c          s1      s2      s3      gammao      a          e0
    1 2417.000  1.410000  0.000  1.000  0.000  0.000  0.000
$#   v0
    1.000
```

Additionally, the equation of state (EOS) needs to be defined, most commonly as a Gruneisen EOS with cubic shock-velocity-particle velocity defining the pressure for compressed materials. The constants in the Gruneisen EOS are found from the shock wave velocity versus particle velocity curve. Two example input cards following the LS-DYNA nomenclature for water (mat_009) are given according to Trevino (2000) and Webster (2007) in Table 16 and Table 17, respectively.

Additionally, Gruneisen EOS is the most commonly used EOS for defining the water behaviour with underwater explosion events. An example input card following the LS-DYNA nomenclature is given in Table 18 according to Webster (2007).

17.2.7 Explosives

An explosive material requires two keywords to define the behaviour of the material. These include the material keyword and the equation of state (EOS). The mechanical properties to be considered are the mass density, the detonation velocity in the explosive and the Chapman-Jouguet pressure. Furthermore, the bulk modulus, shear modulus and yield stress may be required depending on the model.

For the EOS, there are three possibilities to define the pressure for the detonation products. All of these EOS define the pressure as a function of the relative volume and the internal energy per initial volume. The most commonly used EOS for explosive behaviour is the standard Jones-Wilkins-Lee (JWL). This EOS was modified by Baker (1997) and has the added feature of better describing the high-pressure region above the Chapman-Jouguet state.

In addition to the material and EOS definitions in LS-DYNA, the INITIAL_DETONATION keyword is required to define the position and time of the initiation of the detonation process. This is the point at which the detonation initiates and the time for the remaining explosive to detonate is determined by the distance to the centre of the element divided by the detonation velocity. In the material definition for MAT_HIGH_EXPLOSIVE_BURN (mat_008) the value of BETA determines the type of detonation. If beta burn is used, any compression of the explosive material will cause detonation. For programmed burn, the explosive material can act as an elastic perfectly plastic material through the definition of the bulk modulus; shear

Table 19: Explosive material model

```
*MAT_HIGH_EXPLOSIVE_BURN
$# mid      ro      d      pcj      beta      k      g      sigy
    1 1630.000  6930.00  2.1e10  2.000  0.500  0.000  0.000
```

Table 20: Equation of state for the explosive material model

```
*EOS_JWL
$# eosid      a          b          r1      r2      omeg      e0      vo
    1  3.71e11  3.23e9     4.15     0.950  0.300  7.0e9  1.000
```

modulus, and the yield stress. In this case, the explosive must be detonated with the INITIAL_DETONATION keyword.

An example input card following the LS-DYNA nomenclature for TNT (mat_008) is given in Table 19 according to Webster (2007).

Furthermore, the most commonly used Jones-Wilkens-Lee EOS is given in Table 20 according to the LS-DYNA nomenclature (Webster, 2007).

17.2.8 Risers, Umbilical or Power Cable

What all these structures have in common is the fact that they are typically very long, therefore slender. Their global mechanical properties to be defined are the bending-, torsional- and axial stiffness. Furthermore, the main aspect to be covered when modelling such structures is their stiffness dependency with respect to tension, torsion and curvature, i.e. stick-slip effects.

Therefore, experimental measurements of the global and local behaviour as well as a local analysis of the cross-section are needed. Typical numerical implementations would utilize elasto-plastic and visco-elastic material models considering friction, contact formulation (lift-off) as well as torsion/rolling effects on pipes.

Sævik (2011) studied the local behaviour of stresses in flexible pipes with a detailed model considering the cross-section build-up. However, for global analysis of an offshore structure, where the support effect of the slender structure is of interest, a simpler discretisation using beam elements with local stiffness properties can be used, see Rustad *et al.* (2008).

For a typical 8" flexible riser the following global parameters can be found: $EI = 200 \text{ kNm}^2$, $EA = 7.7 \cdot 10^8 \text{ N}$, $GI_t = 5.9 \cdot 10^6 \text{ Nm}^2$.

An example input card following the LS-DYNA nomenclature for a visco-elastic material (mat_117) is given in Table 21.

Table 21: Visco-elastic riser material model

```
*MAT_VISCOELASTIC
$#      mid      ro      bulk      g0      gi      beta
      1  8650.000  2.06e11  0.8e11  0.1e11  0.200
*END
```

17.2.9 Composites

Composite materials can be of various types, such as classical fibre-reinforced plastics or various stacks of materials, i.e. sandwich like structures. Therefore, their material parameters are very specific to the exact type of composite found in the offshore structure.

Menna *et al.* (2011) simulate impact tests of GFRP composite laminates using shells and provide the material parameters for a Mat Composite Failure Option Model (mat_059) of LS-DYNA. Feraboli *et al.* (2011) present an enhanced composite material with damage (mat_054) for orthotropic composite tape laminates together with a series of material parameters.

Most orthotropic elastic materials can be described until failure according to:

$$[C] \{\sigma\} = \{\epsilon\}$$

Table 22: Composite material model

```

*MAT_COMPOSITE_MATRIX
$#      mid      ro
      2 7850.0000
$#      c11      c12      c22      c13      c23      c33      c14      c24
      2.8409E+9 3.3956E+8 1.1319E+9      0.000      0.000 3.9615E+8 7.4958E+7 2.3769E+7
$#      c34      c44      c15      c25      c35      c45      c55      c16
      0.000 8.3506E+6 2.3769E+7 7.9231E+7      0.000 1.6645E+6 5.5485E+6      0.000
$#      c26      c36      c46      c56      c66      aopt
      0.000 2.7731E+7      0.000      0.000 1.9420E+6      0.000
$#      xp      yp      zp      a1      a2      a3
      0.000      0.000      0.000      0.000      0.000      0.000
$#      v1      v2      v3      d1      d2      d3      beta
      0.000      0.000      0.000      0.000      0.000      0.000      0.000
    
```

where C is the compliance matrix besides the six stress and strain components. Hence, the compliance matrix can be composed of the extensional stiffness coefficients, the extensional-bending stiffness coefficients and the bending stiffness coefficients.

An example input card following the LS-DYNA nomenclature for a composite matrix material (mat.117) using such compliance matrix formulation is given in Table 22 for an equivalent stiffened plate.

17.2.10 Concrete

Concrete material requires two keywords to define the behaviour of the material. These include the material keyword and the equation of state (EOS). The mechanical properties to be considered are the mass density, the shear modulus and an appropriate measure of the damage, respectively softening. The EOS describes the relation between the hydrostatic pressure and volume in the loading and unloading process of the concrete uncoupled from the deviatoric response. These parameters are typically obtained by experimental testing of the concrete under different loading directions and rates. Thus, the damage includes strain-rate effects.

Markovich *et al.* (2011) present a calibration model for a concrete damage model using EOS for tabulated compaction and a concrete damage, release 3, model (mat_72r3) and provide the required input parameters. Tai and Tang (2006) studied the dynamic behaviour of reinforced plates under normal impact using the Johnson-Holmquist Concrete equivalent strength model with damage and an EOS, which requires less input parameters and allows for easier implementation with good accuracy.

An example input card following the LS-DYNA nomenclature for concrete material (mat.111) is given in Table 23 according to Tai and Tang (2006).

Table 23: Concrete material model

```

*MAT_JOHNSON_HOLMQUIST_CONCRETE
$#      mid      ro      g      a      b      c      n      fc
      1 2240.000 13.467e11      0.750      1.650      0.007      0.760      48.00
$#      t      eps0      efmin      sfmax      pc      uc      pl      ul
      0.000      1.000      0.010      11.700      13.60      0.00058      1.050      0.100
$#      d1      d2      k1      k2      k3      fs
      0.030      1.000      17.40      38.80      29.80      0.000
    
```

Table 24: Soil material model

```

*MAT_MOHR_COULOMB
$# mid ro gmod rnu phi cval psi
1 1834.862 5.0e06 0.300 0 0.523 5.0e03 0.000
$# nplanes lccpdr lccpt lccjdr lccjt lcsfac
0 0 0 0 0 0
$# gmoddp gmodgr lcgmep lcphiiep lcpstiep lcgmst cvalgr aniso
0.000 0.000 0.000 0.000 0.000 0.000 0.000 1.000000
$# dip dipang cplane frplane tplane shrmax local
0.000 0.000 0.000 0.000 0.000 1.00E+20 0.000
    
```

17.2.11 Soil

For some simulations of hazard the seabed has to be included. However, the material parameters for seabed, respectively soil, are fairly location dependent and may vary significantly within close proximities. Therefore, it is of utmost importance to obtain experimental data for the site in question.

Typically those experiments should identify the soil stiffness in different directions, the friction, the break out resistance and a cycling behaviour (trenching). Henke (2011) presents numerical and experimental results for Niederfelder sand and uses a hypoplastic constitutive model, assuming cohesionless linear elastic behaviour, to achieve good correspondence. Vermeer and Jassmin (2011) use a SPH approach with an elastic-plastic Mohr-Coulomb model to simulate drop anchors and present the utilized material parameters. Furthermore, solid elements can be used to represent sandy soils or granular materials following the Mohr-Coulomb behaviour.

An example input card following the LS-DYNA nomenclature for a Mohr-Coulomb material (mat_173) is given in Table 24 according to the material parameters from Vermeer and Jassmin (2011).

18 BENCHMARK STUDY: RESPONSE OF STIFFENED PANEL SUBJECTED TO HYDROCARBON EXPLOSION LOADS

18.1 Scope of Work

The objective of the Benchmark Study is to compare procedures and the strength assessment results of stiffened steel panels subjected to hydrocarbon explosion loads performed by the members of Committee V.1. The capabilities of modern software to simulate such complex loads and responses are also to be evaluated. Structural response of stiffened steel panels subjected to explosion loads is analysed and compared in particular with respect to:

1. Time-displacement profile at the centre of each panel.
2. Residual deflections at 25 locations over the panel surface.

The benchmark is based on a full scale test experiments carried out at the Spadeadam test site, UK, Figure 24.

Input data regarding geometry of tested panels and results of the tests are obtained by courtesy of The Steel Construction Institute, UK, (SCI, 1998).



Figure 24: Spadeadam test site, offshore module and location of the panel during the test.

The following committee members contributed to the benchmark:

Participation	Affiliation	Analysis software	Reference on Figures
J. Czujko	Nowatec, Norway	LS-Dyna	Nowatec
Wen-Yong Tang	Shanghai Jiao Tong University, China	Abaqus, Dytran	SJTU
M. Riley	Defence R&D (DRDC) Canada	LS-Dyna	DRDC
S. Ehlers	Aalto University, Finland ¹	LS-Dyna	AU

¹ Currently, NTNU, Trondheim, Norway

18.2 Benchmark Model, Geometry

For this benchmark a stiffened panel (Panel 1 from the test) is selected. Geometry of the panel is presented in Figure 25.

18.3 Material data

Material properties derived from coupon tests for panel no.1 are presented in Table 25.

18.4 Loads

A panel loading is provided in the form of idealized representations of the pressure time profiles. For each pressure transducer, the idealized load pulse rise time and duration was calculated. Figure 26 presents representative rise time (T1) and duration (T2) of load pulse.

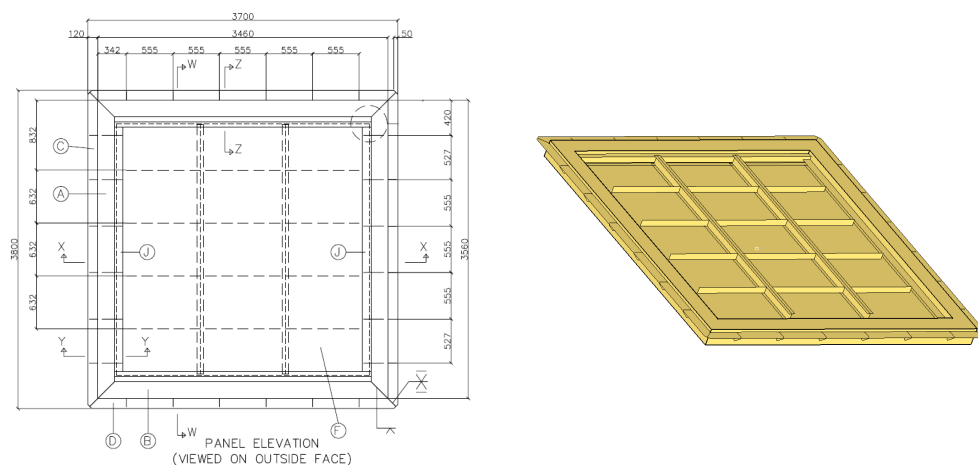


Figure 25: Stiffened panel. Geometry used in the benchmark study.

Table 25: Material properties of the panel.

		Flat Stiffener (75 × 6)	RSJ Stiffener	Plates
Young modulus	<i>MPa</i>	210000	210000	210000
Poisson ratio	-	0.3	0.3	0.3
Yield stress	<i>MPa</i>	270	300	305
Ultimate tensile stress	<i>MPa</i>	477	460	490
Elongation	%	29.9	27.5	28.8
Density	<i>t/mm³</i>	7.85E-009	7.85E-009	7.85E-009

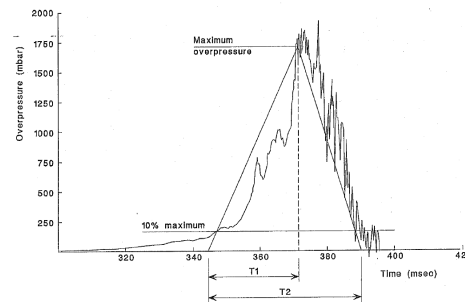
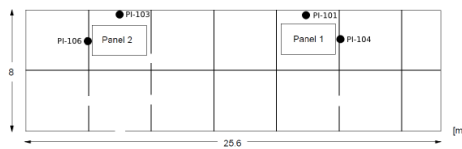


Figure 26: Location of the panel in the test rig and interpretation of the blast overpressure.

The pressure and duration information for each pressure transducer is summarised in Table 26.

18.5 Monitoring of Results

The results of the Benchmark represent transient dynamic response of the test panel and damage of the panel in 25 predefined points, Figure 27.

18.6 Benchmark Procedure

Benchmark study has been carried out in two phases:

1. *Phase 1* where all model development including geometry, boundary conditions, materials and loads was based on individual participants' interpretation of input data from the test.
2. *Phase 2* where assumptions regarding explosion loads were agreed upon between participants of the benchmark study.

In addition, parameter studies involving modelling assumptions regarding representation of geometry, FE mesh density, strain rate effects and application of explosion overpressure have been carried out.

Table 26: Pressure and duration data.

Pressure Transducer ID	Coordinate [m]			Maximum Overpressure [mbar]	Maximum Overpressure > 1 ms duration [mbar]	Time of arrival [ms]	Idealised Profile Representation	
	X	Y	Z				Rise Time [ms]	Duration [ms]
PI-101	18	7.5	7.9	1320	1034	544.3	77.2	110.0
PI-104	20	7.9	6.1	910	792	523.7	51.9	100.7

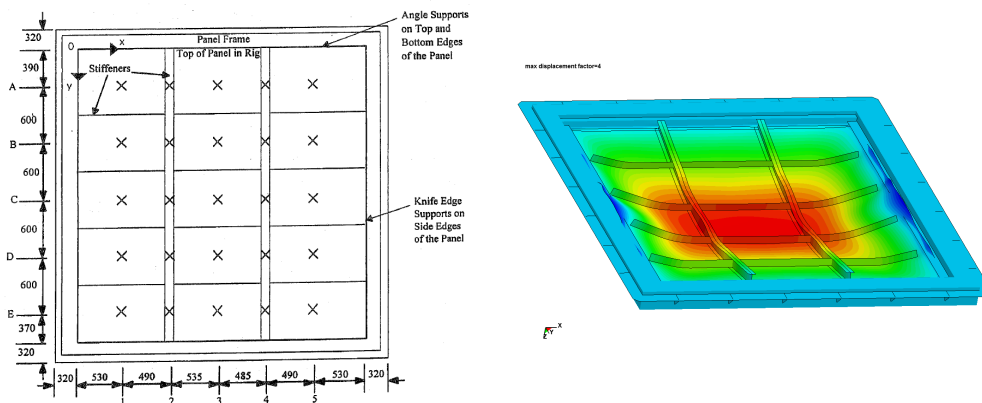


Figure 27: Location of the monitoring points for damage control and final deformation of the panel.

18.7 Phase 1 – Modelling Assumptions and Results

18.7.1 Modelling Assumptions

The following modelling assumptions have been considered:

- Geometry and boundary conditions
- Material properties
- Overpressure magnitude and profile based on input data supplied

Table 27 summarizes the modelling approach of all participants in the benchmark study.

18.7.2 Summary of Results

Transient response

Time response data prepared by modellers is presented in Table 28. Results from AU and SU (ABAQUS) represent upper bound of results. In turn results from Nowatec,

Table 27: Phase 1. Modelling approach for benchmark study.

Panel no.1	Modeller				
	Nowatec (LS-DYNA)	SU (DYTRAN)	SU (ABAQUS)	DRDC (LS-DYNA)	AU (LS-DYNA)
Geometry	full panel	full panel	full panel	full panel	quarter of panel
	with outer frame	without outer frame	without outer frame	with outer frame	with outer frame
BC (knife edge)	with separation	no separation	no separation	with separation	with separation
Material (strain effects)	evaluated	evaluated	evaluated	evaluated	evaluated
Loads	average of P-101 (1 ms) and P-104 (1 ms)	average of P-101 (1 ms) and P-104 (1 ms)	average of P-101 (1 ms) and P-104 (1 ms)	3 zones of pressure	average of P-101 (max) and P-104 (max)
	$P = 913 \text{ mbar}$	$P = 913 \text{ mbar}$	$P = 913 \text{ mbar}$	$B - 910 \text{ mbar}, 51.8 \text{ ms}, 100.7 \text{ ms}$	$P = 1115 \text{ mbar}$
	$T1 = 64.5 \text{ ms}$	$T1 = 64.5 \text{ ms}$	$T1 = 64.5 \text{ ms}$	$E - 1183 \text{ mbar}, 68.8 \text{ ms}, 107.0 \text{ ms}$	$T1 = 64.5 \text{ ms}$
	$T2 = 105.35 \text{ ms}$	$T2 = 105.35 \text{ ms}$	$T2 = 105.35 \text{ ms}$	$F - 636 \text{ mbar}, 34.9 \text{ ms}, 94.5 \text{ ms}$	$T2 = 105.35 \text{ ms}$

Table 28: Summary of max transient deflection predictions as a ratio of observed maximum deflection from test.

	Nowatec	SU (DYTRAN)	SU (ABAQUS)	DRDC	AU
Panel no.1	0.83	0.85	1.05	0.66	1.09

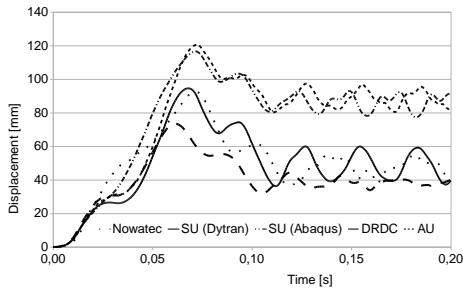


Figure 28: Summary of max transient deflection.

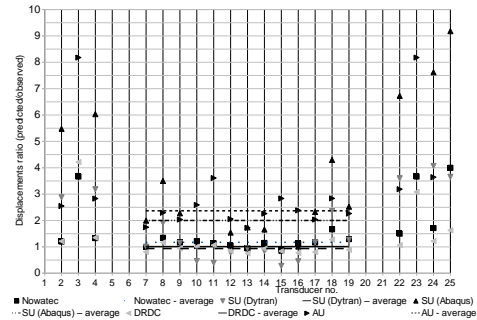


Figure 29: Comparison of residual deflections.

Table 29: Summary of residual deflection predictions as an average ratio of predicted residual deflection vs. measurements.

	Nowatec LS-DYNA	SJTU (DYTRAN)	SJTU (ABAQUS)	DRDC (average) LS-DYNA	AU (average) LS-DYNA
Panel no.1	1.13	1.00	1.99	0.93	2.36

DRDC and SU (DYTRAN) represent lower bound results. Transient response of the panel for Phase 1 is given in Figure 28.

Residual deflections

Residual deflections are presented in Figure 29. All modellers obtained deflections comparable to experiment in measuring points from 7 to 19 that lie in the centre of the panel. All modellers, excluding DRDC, failed to predict deflections in the panel's corners that are close to experimental results.

An average of displacements ratio was calculated to compare predictions between modellers. Results are presented in Table 29.

The closest predictions were obtained by Nowatec, SJTU (DYTRAN) and DRDC. Models analysed by Aalto University and Shanghai Jiao Tong University in ABAQUS over-predicted the residual deflections.

18.8 Phase 2 – Modelling assumptions and results

18.8.1 Unified explosion overpressure

In order to unify modelling of explosion overpressure it has been agreed to repeat benchmark study with overpressure obtained from transducer PI-04 with maximum overpressure 792 mbar.

18.8.2 Summary of results

Transient response

Time response data prepared by modellers are illustrated in Figure 30 and summarised in Table 30. Results compared represent a case where dumping and friction are not

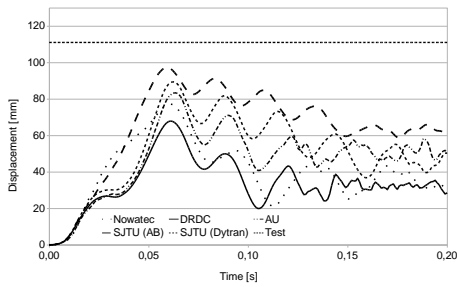


Figure 30: Summary of max transient deflections. Strain rate included.

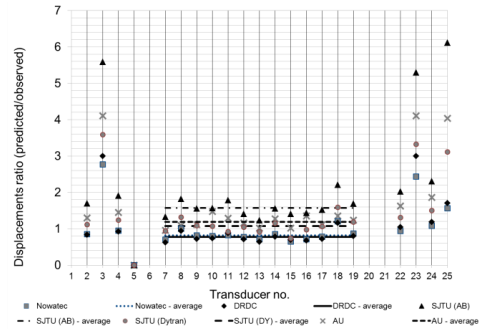


Figure 31: Comparison of residual deflections. Strain rate included.

Table 30: Summary of max transient deflection predictions as a ratio of observed maximum deflection from test.

	Nowatec	SJTU (DYTRAN)	SJTU (ABAQUS)	DRDC	AU
Panel no.1 No strain rate	0.91	1.13	0.93	0.92	0.79
Panel no.1 Strain rate	0.70	0.81	0.88	0.61	0.75

Table 31: Summary of residual deflection predictions as an average ratio of predicted residual deflection vs. measurements.

	Nowatec	SJTU (DYTRAN)	SJTU (ABAQUS)	DRDC	AU
Panel no.1 No strain rate	1.70	2.68	1.64	1.88	1.29
Panel no.1 Strain rate	0.82	1.07	1.57	0.77	1.19

accounted for. Results from SJTU (both DYTRAN and ABAQUS) represent upper bound of results. In turn results from Nowatec and DRDC represent lower bound results. Results from AU give a slightly unusual conservative prediction.

Residual deflections

Residual deflections are presented in Figure 31. All modellers obtained deflections comparable to experiment in measuring points from 7 to 19 that lies in the centre of the panel. All modellers, excluding DRDC, failed to predict deflections in the panel's corners that are close to experimental results.

An average of displacements ratio was calculated to compare predictions between modellers. Results are presented in Table 31.

The best predictions were obtained by AU, SJTU (ABAQUS) and Nowatec. Models analysed by Shanghai Jiao Tong University in DYTRAN over-predict the residual deflections. Further the strain rate dependency does not seem to be considered to the same extent by ABAQUS when compared to DYTRAN and LS-DYNA.

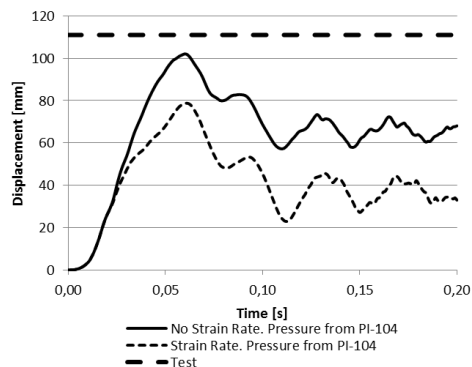


Figure 32: Effects of strain rate obtained for different models.

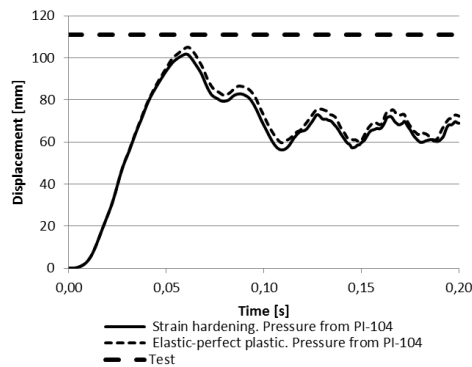


Figure 33: Effects of different material models on panel response.

18.9 Parameter Study

18.9.1 Effects of Strain Rate and Material Models Applied

Different material models: elastic-perfectly plastic and elastic-plastic with hardening, influence the maximum and residual deflections. Strain rate effects have been implemented using Cowper-Symonds equation with $D = 40$ and $P = 5$. Effects of strain rate and different material models applied are illustrated in Figure 32 and Figure 33.

18.10 Conclusion from the Benchmark study

The presented benchmark study consists of a relatively simple structural arrangement, i.e. a stiffened panel supported by a frame, subjected to a hydrocarbon explosion load. However, the study proved to be sufficiently complex to cause significant scatter in results when analysed by a group of experts. This scatter is attributed to the underlying simulation assumptions made by the analysts. These results provide invaluable insight into the variability in predictions when different values are used for influential parameters, one of which is the analysts themselves.

In the first phase the analysts were provided some model details and left to make assumptions which they saw fit. This phase unveiled the influence of the individual approximations including the assumed pressure loading, geometric discretization, and boundary conditions. It was found that ABAQUS and DYNA were able to predict the transient deflection with good accuracy, both for the full panel with and without the outer frame and knife-edge support modelled. However, for the residual deflection neglecting the frame and support or simplifying the applied pressure as the average of the measured pressures caused significant deviation from the full-scale measurements. On the contrary, the lower pressure assumption causes an under-prediction of the transient deflection, but could lead to accurate residual deflections. Furthermore, it is worthwhile to note that only by modelling the asymmetry in the pressure load, the panels' corner deflections can be captured accurately. In experiments the steel material shows a large reduction in deflection from the peak transient value to the residual deflection, which is not accurately described in the numerical material models. Hence, it was found that it is possible to predict either the transient or the residual deflection accurately, but not both with a single simplified model. A detailed strain rate dependent material test and modelling series would bring more light into this phenomenon in the future.

Phase two of this study which defined the load, material properties, and system characteristics (i.e. damping and friction) significantly reduced the variation in the different analysts' results, except for the quarter model, which was overly stiff. The exclusion of strain rate dependency provided poor results compared to experimental measurements and confirms the significant rate dependency of the panel materials. This would have to be known in order to provide more accurate predictions compared to experiments. Additionally, a global geometric model considering the actual supports as well as a more accurate load distribution compared to the experiments would be favourable.

19 REFERENCES

- Adams, N. (2003). *Terrorism & Oil. Penn Well Corp.* Tulsa, OK
- Alashti, R.A, Rahimi, G.H., Poursaeidi, E. (2008). Plastic limit load of cylindrical shells with cut-outs subject to pure bending moment, *Intl. Journal of Pressure Vessels and Piping* 85; 498-506
- Alsos H.S, Amdahl J, Hopperstad O.S.(2009). On the resistance to penetration of stiffened plates, Part II: Numerical analysis. *International Journal of Impact Engineering* 2009;36;875-887.
- Alsos H.S, Hopperstad O.S, Törnqvist R, Amdahl J. (2008). Analytical and numerical analysis of local necking using a stress based instability criterion. *International Journal of Solids and Structures* 2008;45;2042-2055.
- API. (2000), API recommended practice 2A-WSD: Recommended practice for planning, designing and constructing fixed offshore platforms – working stress design. *American Petroleum Institute.*
- API RP 2FB.(2006); “Recommended Practice for the design of offshore Facilities against fire and blast loading”. *American Petroleum Institute.*
- Baker E.L, Stiel L.I. (1997). Improved Quantitative Explosive Performance Prediction Using Jaguar, 1997. *Insensitive Munitions and Energetic Materials Technology Symposium, Tampa, FL, 1997.*
- Barlat F, Maeda Y, Chung K, Yanagawa M, Brem JC, Hayashida Y, Lege DJ, Matsui K, Murtha SJ, Hattori S, Becker RC, Makosey S. (1997). Yield function development for aluminium alloy sheets. *J. Mech. Phys. Solids.* 45, 1997, 1727–1763.
- Berstad T, Hopperstad O.S, Langseth M. (1994). Elasto-viscoplastic constitutive models in the explicit finite element code LS-DYNA3D. *2nd International LS-DYNA3D Conference, San Francisco, Sept 20– 21, 1994*
- Bjerketvedt D., Bakke J.R., Van Wingerden K. (1997). *Gas explosion handbook J Hazardous Materials*, Vol.52 (1):1-150
- Carl, D. & Pontius, T. (2006). Numerical investigations of the influence of the charge geometry on the blast formation. *Proc 19th Military Aspects Blast & Shock*, 1st-6th Oct, Calgary, Canada.
- Clouteau, D., Broc, D., Deve, G., Guyonvarh, V., Massin, P. (2012). Calculation methods of Structure–Soil–Structure Interaction (3SI) for embedded buildings: Application to NUPEC tests. *Soil Dynamics and Earthquake Engineering* 32, 129–142
- Cole, R.H., (1948). *Underwater Explosions, Princeton University Press, New Jersey*
- Cui L, Kiernan S, Gilchrist MD. (2009). Designing the energy absorption capacity of functionally graded foam materials. *Materials Science and Engineering A* 507, 2009, 215–225
- Czujko J. (2001). Design of offshore facilities to resist gas explosion hazard – Engineering Handbook. *CorrOcen* 2001.

- Czujko, J.(2010). Consequences of explosions in various industries in Safety and Reliability of Industrial Products, *System and Structures*, Carlos G. Soares, pp. 107-132.
- DNV DNV-RP-F107.(2001). Risk Assessment of Pipeline Protection, *Det Norske Veritas, Recommended Practice*, March 2001
- DNV-OS-A101, (2008). Safety principles and arrangements. *Det Norske Veritas, Offshore Structures*.
- Do IHP. LS-DYNA ALE. (2009). Advanced Applications Course Notes, April 22-24, 2009, Livermore, CA
- Dolorme L, Inglesias S. A. Perez S. A.(2005). Sloshing Load Simulation in LNG Tankers with SPH, *International Conference on Computational Methods in Marine Engineering MARINE 2005*.
- Ehlers S, Broekhuijsen J, Alsos HS, Biehl F, Tabri K. (2008). Simulating the collision response of ship side structures: A failure criteria benchmark study. *Int Ship Progress 2008*; 55;127-144.
- Ehlers S, Varsta P. (2009). Strain and stress relation for non-linear finite element simulations. *Thin-Walled Structures 2009*; 47; 1203-1217.
- Ehlers S. (2009b). A procedure to optimize ship side structures for crashworthiness. *Journal of Engineering for the Maritime Environment 2009b*; 224: 1-12.
- Ehlers S. (2009a). Strain and stress relation until fracture for finite element simulations of a thin circular plate. *Thin-Walled Structures*, 2009a, 48(1); 1-8.
- EIA (2010). World Energy Demand and Economic Outlook (<http://www.eia.doe.gov/oiiaf/ieo/world.html>)
- Eik K, Gudmestada O.T. (2010). Iceberg management and impact on design of offshore structures. *Cold Regions Science and Technology*. 2010; 63(1-2), 15-28
- FABIG, (2010). Fire Loading and Structural Response, *Technical Note 11, Rev. 2*.
- Falck, A., (2011). Leak frequency modelling for offshore QRA based on the hydrocarbon release database. *FABIG issue 57*.
- Famiyesin, O.O.R., Oliver, K.D., Rodger, A.A. (2002). Semi-empirical equations for pipeline design by the finite element method, *Computers and Structures 80*; 136-1382
- FEMA P646, (2008). *Guidelines for Design of Structures for Vertical Evacuation from Tsunamis*. June 2008.
- Feraboli P Wade B. Deleo F. Rassaian M. Higgins M. Byer A. (2011). LS-DYNA MAT54 modeling of the axial crushing of a composite tape sinusoidal specimen. *Composites: Part A (2011)*, doi:10.1016/j.compositesa.2011.08.004.
- Forsber, J. Hilding, D. Gürtner, A. (2010). A homogenized cohesive element ice model for simulation of ice action a first approach. *5th International Conference on Collision and Grounding of Ships 2010*. Finland.
- Fujita T. (2011). Tsunami Impacting Eastern Japan and Preparedness for Extraordinary Natural Disaster. *Port and Airport Research Institute, Japan*.
- Gao Z., et. al.(2011). Numerical simulation of flooding of a damaged ship, *Ocean Engineering*, 38, 2011
- Geers, T.L. (1978). Doubly Asymptotic Approximations for Transient Motions of Submerged Structures, *The Journal of Acoustical Society of America*, Vol 64, pp. 1500-1508.
- Gielen AWJ. (2008). A PVC-foam material model based on a thermodynamically elasto-plastic-damage framework exhibiting failure and crushing. *International Journal of Solids and Structures 45*, 2008, 1896–1917

- Grau, L.W. (1998). The RPG-7 on the battlefield of today and tomorrow. *Infantry*, May-Aug. pp. 6–8
- Gunaratna, R. (2008). The Threat to the Maritime Domain: How Real is the Terrorist Threat? *Chapter 7 in Armed Groups, Department of the Navy*, 2008
- Hallquist J.O. (2007). LS-DYNA keyword user's manual, Version 971, 2007. Livermore Software Technology Cooperation, California
- Haver, S., (2004A). A Possible Freak Wave Event Measured at the Draupner Jacket. *IFREMER seminar*.
- Haver, S., (2004B). Freak Waves: A Suggested Definition and Possible Consequences for Marine Structures. *IFREMER seminar*.
- Helland, Hermundstad and Stansberg. (2001). Designing for Wave Impact on Bow and Deck Structures. *Proceeding of the Eleventh International Offshore and Polar Engineering Conference*, Stavanger, Norway, June 17-22, 2001.
- Henke, S. (2011). Numerical and experimental investigations of soil plugging in open-ended piles. Ports for container ships of future generations workshop, Hamburg. 2011, 97-122
- Hogström P, Ringsberg J.W, Johnson E. (2009). An experimental and numerical study of the effects of length scale and strain state on the necking and fracture behaviours in sheet metals. *International Journal of Impact Engineering* 2009, 36;1194-1203.
- Hogstrom, P., Ringsberg, J.W. and Johnson, E., (2010). Analysis of a struck ship with damage opening-influence from model and material properties uncertainties. *Proceedings of OMAE-2010*, 20052.
- HSE (2001). Offshore technology report 2001/013 - Loads. <http://www.redorbit.com/news/general/53790/iraqi-oil-terminal-closed-after-attack/>
- Hu, Z., Liu, Z., and Amdahl, J., (2010). Collision character research for semi-submersible through model test, simplified analytical and numerical simulation method. *Proceedings of OMAE-2010*, 20253.
- ISO 19902, (2007). *Fixed steel offshore structures. First edition 2007-12-01*.
- Isshiki, H, Yoon, B. S., Cho, S. R. (2010). A new model for analyzing collision of ships, *Proceedings of the ASME 2010 29th International Conference on Ocean, Offshore and Arctic Engineering, June 6-11, 2010*, Shanghai, China.
- Johnston M, Timco GW, Frederking R, Miles M. (2008). Measuring global impact forces on the CCGS Terry Fox with an inertial measurement system called MOTAN. *Cold Regions Science and Technology*, 2008, 52, 67-82
- Kim, B.J., Seo, J. K., Park, J. H., Jeong, J. S., Oh, B. K., Kim, S. H., Park, C. H., Paik, J. K., (2010). Load characteristics of steel and concrete tubular members under jet fire: An experimental and numerical study. *Ocean Engineering* 37, 2010, pp. 1159–1168.
- Korkut E, Atlar M, Incencik A. (2005). An experimental study of global loads acting on an intact and damaged Ro-Ro ship model, *Ocean Engineering* 32, 2005.
- Lademo O.G, Hopperstad O.S, Berstad T, Langseth M. (2005). Prediction of plastic instability in extruded aluminium alloys using shell analysis and a coupled model of elasto-plasticity and damage. *Journal of Materials Processing Technology* 166 (2005) 247–255.
- Langseth M, Hopperstad O.S, Hanssen A.G. (1998). Crash behaviour of thin-walled aluminium members. *Thin-Walled Structures*. 1998. 32;127–150
- Le Touzé, et. al. (2010). SPH simulation of green water and ship flooding scenarios, *9th International Conference on Hydrodynamics, 2010*, Shanghai, China.
- Lee, J., Rude, G., Paulgaard, G., (2010). Loading Regimes for Close-Proximity Under-

- water Explosions, *Proceedings of the 81st Shock and Vibration Symposium*, Orlando, FL
- Lee, J.J., Smith, M.J., Huang, J., and Paulgaard, G.T.(2008). Deformation and rupture of thin steel plates due to cumulative loading from underwater shock and bubble collapse, *Proceedings of the 79th SAVIAC Shock and Vibration Symposium*, Orlando, FL
- Lemaitre J. (1992). A Course on Damage Mechanics, *Springer-Verlag*, 1992.
- Lin, Y.,Feng, G., Ren, H., and Yu, H. (2010).Research on collision strength for deep sea submersible structures, *Proceedings of OMAE-2010*, 20665.
- Lindholm U.S, Bessey R.L, Smith G.V. (1971). Effect of strain rate on yield strength, tensile strength and elongation of three aluminium alloys. *J. Mater. JMLSA* 1971;6(1):119–33.
- Liu Z, Amdahl J, Løset S. (2011). Plasticity based material modelling of ice and its application to ship-iceberg impacts. *Cold Regions Science and Technology*, 2011; 65, 326-334.
- Markovich N, Kochavi E, Ben-Dor G. (2011). An improved calibration of the concrete damage model. *Finite Elements in Analysis and Design*, 2011; 47, 1280–1290
- Martec Limited. (2007). Numerical Study of Soil Modelling Approaches using LS-DYNA. (DRDC Valcartier CR 2008-005). *Defence R&D Canada Valcartier*. Unclassified.
- Medonos, S., Ramman, R. (2009). Why ISO 13702 and NFPA 15 standards may lead to unsafe design. *FABIG Newsletter Issue 53*.
- Menglin, L., Huaifeng, W., Xi, C., Yongmei, Z. (2011). Structure–soil–structure interaction: Literature review. *Soil Dynamics and Earthquake Engineering* 31, 1724–1731.
- Menna, C., Asprone, D., Caprino, G., Lopresto, V., Prota, A. (2011). Numerical simulation of impact tests on GFRP composite laminates. *International Journal of Impact Engineering*, 2011; 38, 677-685.
- Ming P., Duan W.(2011). Numerical simulation of sloshing in rectangular tank with VOF based on unstructured grids, *Journal of Hydrodynamics*, 2010, 22(6):856-864.
- Moan T.(2005).Safety of offshore structures. *Centre for Offshore Research & Engineering. National University of Singapore*.
- Moan T.(2007).Development of Accidental collapse Limit State Criteria for Offshore Structures. *Special Workshop on Risk Acceptance and Risk Communication.March 26-27, 2007, Stanford University*.
- Moan T.(2009).Development of accidental collapse limit state criteria for offshore structures. *Structural Safety, Elsevier*. 2009.
- Négre P, Steglich D, Brocks W. (2004). Crack extension in aluminium welds: a numerical approach using the Gurson–Tvergaard–Needleman model. *Engineering Fracture Mechanics* 71, 2004, 2365–2383.
- Norsok Standard N-004.(2004). Design of Steel structures, *Norwegian Technology Standards*, Oslo, Norway.
- Norsok Standard N-003.(2007). Actions and Action Effects, *Norwegian Technology Centre*, Oslo, Norway.
- Norsok Standard Z-013.(2001). Risk and emergency preparedness analysis, Rev 2, 2001-09-01. *Norwegian Technology Centre*, Oslo, Norway.
- NorsokStandard S-001.(2008). Technical Safety. *Norwegian Technology Centre*, Oslo, Norway.

- NorsokStandard Z-013 (2010). Risk and emergency preparedness analysis. *Norwegian Technology Centre*, Oslo, Norway.
- Nurick, G.N., Martin, J.B. (1989). Deformation of thin plates subjected to impulsive loading—a review, *Part II: experimental studies, International journal of impact Engineering, Vol. 8*, pp. 171-186
- O’Sullivan, T. (2005). External terrorist threats to civilian airlines: a summary of risk analysis of MANPADS, other ballistic weapon risks, future risks, and possible countermeasure policies. *CREATE Report #05-009*, Los Angeles, CA.
- Ong, L.S., Lu, G. (1996). Collapse of Tubular Beams Loaded by a Wedge-shaped Indenter, *Experimental Mechanics, Vol. 36, No 4*.
- Pahos, S.J. (2008). An explicit analysis of a ROPAX vessel under impulsive loading from a VBIED Proc. *ASNE Symp. Shipbuilding in Support of the GWOT Apr. 14-17*, Biloxi, MS.
- Pahos, S.J. (2011). The ballistic response of cross-stiffened panels from a rocket-propelled grenade. *Naval Engineers Journal, Vol. 123*, pp. 55-65.
- Paik, J. K. (2007). Practical techniques for finite element modelling to simulate structural crashworthiness in ship collision and grounding (Part I: Theory). *Ships and Offshore Structures 2007*; 2:1; 69-80.
- Paik, J. K., Czujko, J. (2011A). Assessment of hydrocarbon explosion and fire risks in offshore installations: recent advances and future trends. *The IES Journal Part A: Civil & Structural Engineering, Vol. 4, No. 3, August 2011*, pp. 167–179.
- Paik, J. K., Czujko, J. (2011B). Assessment of hydrocarbon explosion and fire risk in offshore installations: recent advances and future trends. *OMAE2011-49445*.
- Paik, J. K., Czujko, J., Kim, B. J., Seo, J. K., Ryu, H. S., Ha, Y. C., Janiszewski, P., Musial, B. (2011). Quantitative assessment of hydrocarbon explosion and fire risks in offshore installations. *Marine Structures 24, 2011*, pp. 73–96.
- Paik, J. K., Kim, B.J., Jeong, J.S., Kim, S.H., Jang, Y.S., Kim, G.S., Woo, J.H., Kim, Y.S., Chun, M.J., Shin, Y.S., Czujko, J. (2010). CFD simulations of gas explosion and fire actions. *Ships and Offshore Structures, Vol. 5, No. 1, 2010*, pp. 3–12.
- Paik, J., Czujko, J. (2011C). Explosion and Fire Engineering of FPSO (EFEF JIP), Definition of Design Fire Loads. *FABIG Newsletter Issue 58*.
- Peschmann J. (2001). Energy absorption computations of ship steel structures under collision and grounding (translated from German). *Doctoral Dissertation. Technical University of Hamburg 2001*.
- Pill, I., Tabri, K. (2009). Finite element simulations of ship collisions: A coupled approach to external dynamics and inner mechanics, *Proceedings of Analysis and Design of Marine Structures; The 2nd International Conference*, Lisbon, Portugal.
- Polojärvi, A. Tuhkuri, J. (2009). 3D discrete numerical modelling of ridge keel punch through tests. *Cold Regions Science and Technology, Volume 56, Issue 1, April 2009*, Pages 18-29.
- Poonaya, S., Thinwongpituk, C., Teeboonma, U. (2007). An Analysis of Collapse Mechanism of Thin-walled Circular Tubes Subjected to Bending, *Intl. Journal of Mechanical, Industrial and Aerospace Engineering 1:3*
- Qiu, G., and Grabe, J., (2010). Numerical investigation of a ship collision with waterway embankments, *Proceedings of OMAE-2010*, 20363.
- Rajendran, R. (2008) Reloading effects on plane plates subjected to non-contact underwater explosions, *Journal of Materials Processing Technology, Vol. 206*, pp. 275-281

- Rajendran, R., Narasimhan, K. (2001). *Journal of Materials Engineering and Performance*, Vol. 10, No. 1, pp. 66-74.
- Riley, M., Lee, J. and Smith, M.(2010). Bubble Formation and Collapse Characteristics for Close Proximity Underwater Explosions, *Proceedings of the 81st Shock and Vibration Symposium, Orlando, Florida*, October, 15 pages.
- Riley, M.J., Paulgaard, G.T., Lee, J.J., and Smith, M.J.(2009). Failure Mode Transition in Air-backed Plates from Near Contact Underwater Explosions, *Journal of Shock and Vibration*, 28 pages.
- Riska, K. (1987). Modelling ice load during penetration into ice, Joint report of the technical research center of Finland and the National Research Council of Canada, 1987.
- Ritch R, Frederking R, Johnston M, Brown R, Ralph F. (2008).Local ice pressures measured on strain gauge panel during the CCGS Terry Fox bergy bit impact study. *Cold Regions Science and Technology*, 2008, 52, 29-49
- Rosqvist, T, Nyman, T., Sonninen, S., Tuomen, R. (2002).The implementation of the VTMISS system for the Gulf of Finland – a FSA study, *Proc. RINA Intl. Conf. on Formal Safety Assessment*, London.
- Rustad A.M, Larsen C.M, Sørensen A.J. (2008). FEM modelling and automatic control for collision prevention of top tensioned risers, *Marine Structures*, 2008; 21, 80–112.
- Sævik S. (2011). Theoretical and experimental studies of stresses in flexible pipes. *ComputStruct* (2011), doi:10.1016/ j.compstruc.2011.08.008.
- Santos, T.A. GuedesSoares C. (2009).Numerical Assessment of Factors Affecting the Survivability of DamagedRo-Ro Ships in Waves. *Ocean Engineering*.
- Scharrer M, Zhang L, Egge ED. (2002). Collision calculations in naval design systems, *Report. Final report MTK0614 Nr. ESS2002.183, Version 1/2002-11-22, Germanischer Lloyd*, Hamburg 2002.
- Schraad M.W, Harlow F.H. (2006). *International Journal of Solids and Structures* 43 (2006) 3542–3568.
- SCI, (1998).Structural Response Model Evaluation. Blast and Fire Engineering Project – Phase 2. *Report to Joint Industry Project. Document RT681, Version 2*.
- Serco Assurance.(2003). Ship/Platform Collision Incident Database, *Health and Safety Executive, Research Report 053*.
- Ship Structures Committee, report SSC-445. (2005). Structural survivability of modern liners, 2005, (www.shipstructure.org)
- Ship Structures Committee, report SSC-r336. (1990). Liquid sloshing in cargo tanks, 1990, (www.shipstructure.org)
- Suyuthi and Haver S. (2009). Extreme Loads due to Wave Breaking Against Platform Column. *Proceeding of the Nineteenth International Offshore and Polar Engineering Conference, Osaka, Japan, June 21-26, 2009*.
- Tai Y-S, Tang C-C.(2006). Numerical simulation: The dynamic behavior of reinforced concrete plates under normal impact. *Theoretical and Applied Fracture Mechanics*, 2006; 45, 117–127.
- Thinwongpituk, C. Poonaya, S., Choksawadee, S., Lee, M. (2008).The Ovalisation of Thin-walled Circular Tubes Subjected to Bending, *Proceedings of the World Congress on Engineering, Vol. II*.
- Törnqvist R. (2003). Design of crashworthy ship structures.*PhD Dissertation, De-*

- partment of Naval Architecture and Offshore Engineering, Technical University of Denmark 2003.*
- Trevino, T. (2000). Application of Arbitrary LagrangianEulerian (ALE) Analysis Approach to underwater and Air Explosion Problems, *Master's Thesis, Naval Post-graduate School, September 2000.*
- Tsai, S. (1971).A general theory of strength for anisotropic materials. *Composite Materials 1, 1971.*
- UKOOA. (2003A). Fire and explosion guidance, *Part 1: Avoidance and mitigation of explosions. Issue 1.*
- UKOOA. (2003B). Fire and explosion guidance, *Part 2: Avoidance and mitigation of fires.*
- UKOOA, (2003).Guidelines for Ship/Installation Collision Avoidance, *UK Offshore Operators Association.Issue 1, February 2003.*
- Van Raaij and Gudmestad.(2007). Wave-in-deck loading on fixed steel jacket decks. *Marine Structures 20, 2007, 164-184.*
- Van Raaij. (2005). Dynamic behaviour of jackets exposed to wave-in-deck forces. *Dr.ing. dissertation. University of Stavanger, Norway, 2005.*
- Vermeer, P., Jassim I. (2011). On the dynamic elastoplastic material point method. *Ports for container ships of future generations workshop, Hamburg. 2011, 137-152.*
- Voogt and Buchner. (2004). Prediction of wave impact loads on Ship-type Offshore Structures in Steep Fronted Waves. *MARIN Wageningen, Netherlands, 2004.*
- Wang, G. and Spong, R. (2003). Experience based data for FPSO's structural design, OTC 15068, *Offshore Technology Conference, Houston, TX, 5-8 May 2003.*
- Wang, G., Jiang, D.J. and Shin, Y. (2003).Consideration of collision and contact damage risks in FPSO structural designs, *OTC-15316, Offshore Technology Conference, Houston, TX, 5-8 May 2003.*
- Wang, Q.X., Yeo, K.S., Khoo, B.C., Lam, K.Y.(1996a).Strong interaction between a buoyancy bubble and a free surface. *Theoretical and Computational Fluid Dynamics, Vol 8, No. 3, pp. 73-88.*
- Wang, Q.X., Yeo, K.S., Khoo, B.C., Lam, K.Y.(1996b). Nonlinear interaction between gas bubble and free surface, *Computers and Fluids, Vol. 25, No. 7, pp. 607-628.*
- Webster, K.G. (2007). Investigation of Close Proximity Underwater Explosion Effects on a Ship-Like Structure Using the Multi-Material Arbitrary LagrangianEulerian Finite Element Method, *Master's Thesis, Virginia Polytechnic Institute and State University, January 2007.*
- Wierzbicki, T., Suh, M.S. (1988). Indentation of tubes under combined loading, *International Journal of Mechanical Sciences 30 (3-4); pp. 229-248*
- WIKIPEDIA (2010). Rogue wave.
- Yao, X-L., Guo, J., Feng, L-H, Zhang, A-M.(2009). Comparability research on impulsive response of double stiffened cylindrical shells subjected to underwater explosion. *International Journal of Impact Engineering, 36, pp. 754-762.*
- Yoo CH, Kim KS, Choung J, Shim CS, Kang JK, Kim DH, Suh YS, Shim YL, Urm HS, Kim MS, An GB. (2011). An experimental study on mechanical, fatigue and crack propagation properties of IMO type B CCS materials at room and cryogenic temperatures. *Advances in Marine Structures, 2011; pp. 527-535.*
- Yoon, B.S, Cho, R., Isshiki, H. (2009).New Approach for Analyzing Collision of Ships, *Proceedings of OMAE-2009, 79309.*
- Zhang, A-M, Yao, X-L.(2008). Interaction of underwater explosion bubble with com-

plex elastic-plastic structure. *Applied Mathematics and Mechanics – English edition, Vol. 29, No 1*, pp. 89-100.

Zhang, S. (1999). The Mechanics of Ship Collisions, *PhD Thesis, Technical University of Denmark*.

Zhang, S., Ocakli, H. and Pedersen, P.T. (2004). Crushing of ship bows in head-on collision, *International Journal of Maritime Engineering, Transactions of the Royal Institution of Naval Architects, 146: A2*, 39-46.

Zhang, Y.L., Yeo, K.S., Khoo, B.C, Wang, C.(2001). 3D jet impact and toroidal bubbles. *Journal of Computational Physics, Vol. 166, No. 2*, pp. 336-360.

